NASA Contractor Report CR-201151

Report on the Installation and Evaluation of the Mesoscale Atmospheric Simulation System (MASS)

Prepared By:
Applied Meteorology Unit

Prepared for:
Kennedy Space Center
Under Contract NAS10-11844

NASA
National Aeronautics and
Space Administration

Office of Management

Scientific and Technical
Information Program

1996

Attributes and Acknowledgments:

NASA/KSC POC:
Dr. Francis J. Merceret
TM-SPO-3

Applied Meteorology Unit (AMU)

John T. Manobianco, primary author
Randolph J. Evans
Winifred C. Lambert
Gregory E. Taylor
Mark M. Wheeler
Ann M. Yersavich

Table of Contents

Table of Contents

(continued)

List of Illustrations

List of Tables

Executive Summary

The objective of this report is to describe the Applied Meteorology Unit's (AMU) installation and evaluation of the Mesoscale Atmospheric Simulation System (MASS). The National Aeronautics and Space Administration (NASA) funded Mesoscale Environmental Simulations and Operations (MESO), Inc. through a Small Business Innovative Research (SBIR) Phase II contract to develop a version of MASS configured specifically for short-range forecasting at the Kennedy Space Center (KSC) and Cape Canaveral Air Station (CCAS). The implementation of a local, mesoscale modeling system such as MASS at KSC/CCAS is designed to provide detailed short-range (< 24 h) forecasts of winds, clouds, and hazardous weather such as thunderstorms. Short-range forecasting is a challenge for daily operations, and manned and unmanned launches since KSC/CCAS is located in central Florida where the weather during the warm season is dominated by mesoscale circulations like the sea breeze.

At the completion of the SBIR Phase II project in March 1993, MESO, Inc. delivered the MASS software, a Stardent 3000 computer to run MASS, and a final project report. MASS is composed of an initialization module, a dynamical model, and a set of statistical models that generate probability forecasts of specific weather events from dynamical model output and observations. The data used to initialize MASS are obtained from the Meteorological Interactive Data Display System (MIDDS) at the Eastern Range. When MASS was delivered to the AMU, the system did not contain software to reformat and ingest data from MIDDS. The AMU developed and tested routines to reformat MIDDS data and read these data into MASS as part of the overall system checkout and installation.

Beginning in January 1994, the AMU began running MASS twice daily on the Stardent 3000 workstation and archiving model output and observations for the model evaluation. The AMU developed a MASS model evaluation protocol that included objective and subjective verification of forecasts as well as real-time evaluation of model output by forecasters and meteorologists at Range Weather Operations (RWO), Spaceflight Meteorology Group (SMG), and National Weather Service, Melbourne (NWS MLB).

The real-time run statistics from January to October 1994 showed that MASS is extremely robust and would be a very reliable operational system. In general, the evaluation revealed that MASS had no severe biases and did not produce unrealistic forecasts. The AMU's objective verification at Florida rawinsonde sites revealed that MASS predicted the large-scale features as well as the Nested Grid Model. However, 11 km MASS runs did not show more skill than operational models in forecasting warm season precipitation. In addition, the current version of the MASS model output statistics is not suitable for use as a forecasting tool. Finally, the real-time evaluation of model output by RWO, SMG, and NWS MLB found that MASS was occasionally more useful than National Centers for Environmental Prediction (NCEP) models for short-range forecasting. SMG also noted several instances where MASS was far off base and could have adversely affected SMG forecasts.

Based on results from all components of the MASS evaluation, RWO, SMG, and NWS MLB reached a consensus that the AMU should terminate all work with MASS. This consensus was based primarily on the fact that the current version of MASS did not provide sufficient added value over NCEP models to justify the cost of continuing the evaluation with the intent to transition MASS for operational use. It is important to point out, however, that the results of the real-time evaluation by RWO, SMG, and NWS MLB may not be completely representative of the model's capabilities since each group was only able to examine a limited number of cases using a very small fraction of available model output.

This report concludes with the AMU's recommendations for making MASS a cost-effective system. The recommended enhancements focus primarily on upgrades to the software and changes to the real-time run configuration. In order to make substantial improvements in warm season explicit precipitation forecasts, it is likely that deficiencies with respect to model resolution, model physics, and initialization data would need to be corrected. The data available from WSR-88D radars, 915 MHz wind profilers, Radio Acoustic Sounding Systems (RASS), satellites (GOES-I, J and Global Positioning System), and soil moisture probes may offer the opportunity to improve initialization and short-range forecasts by MASS if they can be incorporated into the system in real-time. However, these modifications and changes to MASS will not necessarily improve the utility of forecasts to the point where they will always have added value over NCEP models. The major advantages of running a local mesoscale model are that it can be tailored specifically for forecasting problems and users can choose various parameters of the model configuration and types of data used for model initialization. Nevertheless, these benefits must be weighed against the life-cycle costs and expertise needed to maintain a local modeling system.

The AMU's work on the installation and evaluation of MASS spanned nearly 3 years from early 1993 through the end of 1995. During that time, the AMU learned a number of lessons about the evaluation, application, and utility of local mesoscale models. Specifically, the evaluation protocol for MASS could have included more benchmarking with existing NCEP models, more phenomenological verification, and daily, real-time forecasting by AMU personnel. In addition, the AMU could have provided more thorough familiarization and training on MASS for RWO, SMG, and NWS MLB prior to the subjective evaluation. Finally, MASS model output should have been distributed as gridded fields rather than image products so that users could select the variables, contour intervals and colors, cross section paths, etc.

The AMU will continue to run an updated version of MASS on a non-interference, no-additional-labor basis and send output to MIDDS. The plan is to run one 24-h 11 km forecast on the AMU's IBM RS/6000 Model 390 using an updated version of the software. The primary reason for continuing the MASS runs is to give RWO, SMG, and NWS MLB the opportunity to conduct additional, informal evaluation over a larger number of cases than was possible during 1995. The AMU also identified a number of deficiencies affecting the modeling task that should all be remedied by March 1997 as part of RWO's plan to upgrade MIDDS. At that time, there is the possibility that the AMU could be tasked to resume work with MASS especially if further examination of MASS by RWO, SMG, or NWS MLB reveals that it has more added value that was not discovered as part of their limited subjective evaluation performed during the 1995 warm season.

1.0   Introduction

1.1 Background

The National Aeronautics and Space Administration (NASA) and United States Air Force (USAF) have been conducting ground and spaceflight operations at the Kennedy Space Center (KSC) and Eastern Range at Cape Canaveral Air Station (CCAS) since the early 1960's. Weather support to operations at KSC/CCAS requires detailed forecasts of winds, clouds, ceilings, fog, and hazardous weather such as thunderstorms. Forecasting these parameters for KSC/CCAS is a challenging task since the central Florida facilities are located in an environment where there is an absence of significant large-scale dynamical forcing during much of the year. Under these conditions, regional and local factors such as land/water boundaries, land-use, vegetation type/density, and soil moisture play a dominant role in determining the short-term evolution of weather conditions (Pielke et al. 1991; Xian and Pielke 1991; McCumber and Pielke 1981). Hence, guidance from current generation global and regional models is of limited value for these forecasting problems.

The implementation of mesoscale modeling systems locally at KSC/CCAS is ultimately intended to provide accurate forecasts of specific thunderstorm-related phenomena such as lightning, precipitation, and high winds. These forecasts are important for reducing downtime due to false weather advisories and alerts and minimizing the impact on personnel and equipment due to hazardous weather events occurring without warning. Improved forecast reliability may also permit safe relaxation of weather-related launch commit criteria for manned and unmanned space launches and flight rules for Shuttle landings.

State-of-the-art mesoscale modeling systems typically contain detailed physical parameterizations and are run at very high horizontal and vertical resolutions. As a result, the models require large memory and processing capabilities, and until recently, could only be run on the fastest supercomputing platforms. However, the development of computer workstations during the past 5 years with sufficient memory and processing speed has permitted mesoscale models to generate real-time forecasts at a fraction of the financial cost that would be required to run these models on mainframe supercomputers (Buzbee 1993).

To meet the forecasting needs at KSC/CCAS, NASA funded Mesoscale Environmental Simulations and Operations (MESO), Inc. through a Small Business Innovative Research (SBIR) Phase II contract to develop a version of the Mesoscale Atmospheric Simulation System (MASS) configured specifically for short-range forecasting in the vicinity of KSC/CCAS. The version of MASS developed to support operational weather forecasting at KSC/CCAS was designed to run in real-time on high performance workstations. At the completion of the SBIR Phase II project in March 1993, MESO, Inc. delivered the MASS software, a Stardent 3000 computer to run MASS, and a final project report entitled "Development of a Mesoscale Statistical Thunderstorm Prediction System" (Zack et al. 1993).

1.2 Applied Meteorology Unit Tasking

Under the Mesoscale Modeling Task (005), Subtask 2, the Applied Meteorology Unit (AMU) evaluated MASS to determine its utility for operational weather support to ground and spaceflight operations. At the conclusion of the evaluation, the AMU was also tasked to recommend, develop, and implement any modifications to make MASS suitable to transition for operational use.

1.3 Purpose and Organization of the Report

This purpose of this report is to document the AMU's installation and evaluation of the MASS. Section 2 describes the MASS pre-processor, the dynamical and statistical models, the real-time configuration for the system, and the evaluation protocol. The results of the MASS evaluation are summarized in Section 3. Section 4 focuses on lessons learned regarding the evaluation of a local mesoscale modeling system like MASS, the AMU's recommendations for improving the system, and the reasons why MASS is not yet suitable to transition for operational use. Finally, Section 5 highlights the possibilities for future work with MASS.

2.0 MASS Components and Evaluation Protocol

This section describes the components of MASS, the real-time configuration used to run the pre-processor and model in the AMU, and the evaluation protocol developed by the AMU. The version of MASS developed by MESO, Inc. for NASA under the SBIR Phase II contract and delivered to the AMU is composed of three main components: (1) an initialization module, (2) a dynamical model, and (3) a set of statistical models that generate probability forecasts of specific weather events from dynamical model output and observations. The initialization module and dynamical model are summarized in Tables 2.1 and 2.2, respectively.

2.1. Initialization Module

The initialization module or data pre-processor performs surface parameter specification and surface and atmospheric variable initialization. The surface parameter routines determine the model horizontal grid structure and specify non-prognostic parameters such as terrain height, land/water classification, land use, and fraction of the surface covered by vegetation. The data sources and resolutions used to initialize these parameters are given in Table 2.1.

There are a number of in-situ and remotely-sensed data sources that are presently used to initialize the MASS. The gridded data from the National Centers for Environmental Prediction (NCEP) Nested Grid Model (NGM) C-grid provides first-guess fields for a Barnes (1964) objective analysis of rawinsonde data. The raw NGM C-grid data available at KSC/CCAS have a horizontal spacing of 1.25˚ latitude x 2.5˚ longitude on 10 mandatory pressure levels from 1000 mb to 100 mb. MASS incorporates surface data including measurements of temperature, winds, moisture and clouds from land-based stations, ships, buoys, and wind, temperature and dew point temperature from the mesoscale network of instrumented towers surrounding KSC/CCAS. The surface data are objectively analyzed to the model grid using a two-pass Barnes (1964) objective analysis scheme. The locations of available rawinsonde, surface, buoy, ship, and KSC/CCAS tower observations at initialization time for a typical model run are shown in Figures 2.1 and 2.2.

The three-dimensional initial moisture analyses are enhanced by creating synthetic relative humidity (RH) fields from a combination of manually digitized radar (MDR) data, visual surface-based cloud observations, and infrared satellite data. The scheme consists of three basic steps and is described in MESO (1993) and Young and Zack (1994).

Table 2.1.   MASS initialization module attributes

Attribute	Description	Resolution	Reference
Terrain	US Central Intelligence Agency (CIA) global data set	5 minute	---
Land use / land cover	US Geological Survey Anderson Level II classification scheme	30 seconds (~1 km)	Anderson et al. (1976)
Vegetation	Advanced Very High Resolution Radiometer (AVHRR) data used to compute Normalized Difference Vegetation Index (NDVI)	1 km	Chang and Wetzel (1991)
Soil moisture	Analysis based on Antecedent Precipitation Index (API) using all available precipitation observations for 1-30 days prior to initialization[1]	Variable (depending on available data)	---
Soil temperature	Analysis based on air temperature observations typically for 3 or more days prior to initialization[2]	Variable (depending on available data)	---
Sea surface temperature (SST)	Global monthly climatology used as first guess for analysis of SST observations	Global data set (1 degree)	---
Objective analysis	Barnes Optimum Interpolation (OI)[3]	---	Barnes (1964) OI (Gandin 1963)
Data quality control	Gross error check for unrealistic observations; Hydrostatic consistency ensured by building heights from analyzed surface pressures and virtual temperatures	---	---

[1]Presently initialized to a constant value of 0.2

[2]Presently initialized to surface temperature

[3]Presently used only for sea surface temperature analysis

In the first step, synthetic RH values are derived from surface observations of cloud and current weather as well as pilot reports of clouds. In order to obtain RH values from surface cloud and weather observations, statistical equations which relate visual observations of clouds and weather to vertical RH profiles were developed from a database of co-located surface and rawinsonde observations. A RH-height relationship with a vertical resolution of 25 mb was derived for each cloud/weather category (e.g. middle overcast with precipitation) using the observed cloud base heights as predictors. An objective analysis scheme is used to blend these synthetic RH values with RH measurements using a first guess grid point field of RH.

The second step uses IR radiance data to estimate the fractional cloud coverage and cloud top height distribution in each model grid cell. Cloud base is estimated from the cloud observations at the nearest surface station. Model grid points are then moistened or dried depending on the fractional cloud coverage through the use of the same RH-cloud fraction relationship used to diagnose clouds in the dynamical model.

In the third step, grid cells with precipitation are identified using MDR reports of echo intensity and areal coverage of precipitation and the location of convective towers determined from the IR satellite data following Adler and Negri (1988). The grid cells with diagnosed precipitation are brought to near saturation from the cloud top to the surface of the earth.

Table 2.2.   MASS model attributes

Attribute	Description	Reference
Boundary layer physics	High resolution Blackadar	Zhang and Anthes (1982)
Surface energy and moisture budget	Force-restore model Three-layer soil moisture budget equation (Cover layer and two soil layers)	Noilhan and Planton (1989); Mahrt and Pan (1984)
Grid scale precipitation physics	Diagnostic - condense water vapor in excess of supersaturation[1]	---
	Prognostic - conservation equations for cloud water (ice) and rain water (snow) including cloud microphysics[2]	Zhang (1989)
Sub-grid scale precipitation physics	Kuo-type with moist convective scale downdrafts[3] OR	Kuo (1965); Anthes (1977); Frank and Cohen (1987)
	Fritsch-Chappell with modifications by Zhang and Fritsch	Fritsch and Chappell (1980); Zhang and Fritsch (1986)
Radiation physics	Free atmosphere short and long wave radiation	Sasamori (1972); Stephens (1978); Savijarvi (1990)
Lateral boundary conditions	Blending with Kreitzberg-Perkey sponge condition[3] OR	Perkey and Kreitzberg (1976)
	Radiative	Orlanski (1976)
Data assimilation	Newtonian relaxation	Stauffer and Seaman (1990); Stauffer et al. (1991)

[1]Used for all 45 km simulations
[2]Used for all 11 km simulations
[3]Used for all 11 km and 45 km simulations

2.2. Dynamical Forecast Model

The dynamical forecast model used in this system is version 5.6 of the MASS model. It is a hydrostatic three-dimensional primitive equation model that is a descendent of version 2.0 described by Kaplan et al. (1982). The attributes of the MASS model are summarized in Table 2.2. A detailed description of version 5.6 and specific enhancements to MASS developed for application to forecasting at KSC/CCAS are provided elsewhere (MESO 1993).

The KSC/CCAS real-time version of the model is run with a coarse grid spacing of 45 km (55 x 50 points) covering the southeastern United States and a fine grid spacing of 11 km (45 x 60 points) covering the Florida peninsula, and the eastern Gulf of Mexico, and western Atlantic Ocean. The extent of the 45 km and 11 km domains is shown in Figures 2.1 and 2.2. The vertical spacing of the model's 20 sigma layers used for both coarse and fine grid runs varies from ~20 m at the lower boundary (i.e. the surface) to ~2 km at the upper boundary (i.e. 100 mb).

45 km MASS Grid
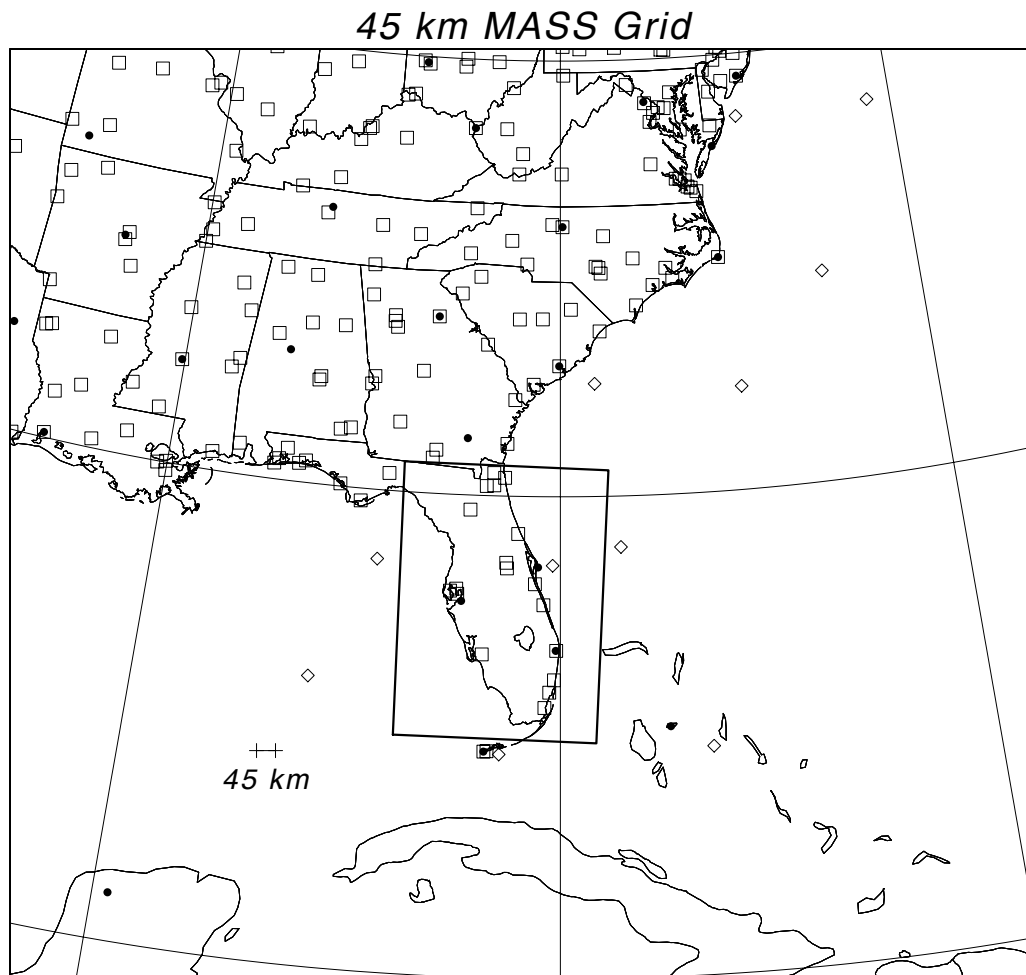
45 km

Figure 2.1. Depiction of the geographical domain covered by the horizontal grid matrices used in the 45 km (coarse grid) mesoscale simulations. An expanded view of the 11 km domain given by the inner rectangle is shown in Figure 2.2. A representative 45 km grid interval is labeled. The locations of available data for typical coarse grid model runs are shown as solid dots for rawinsondes, open squares for surface stations, and open diamonds for ships and buoys.

11 km MASS Grid
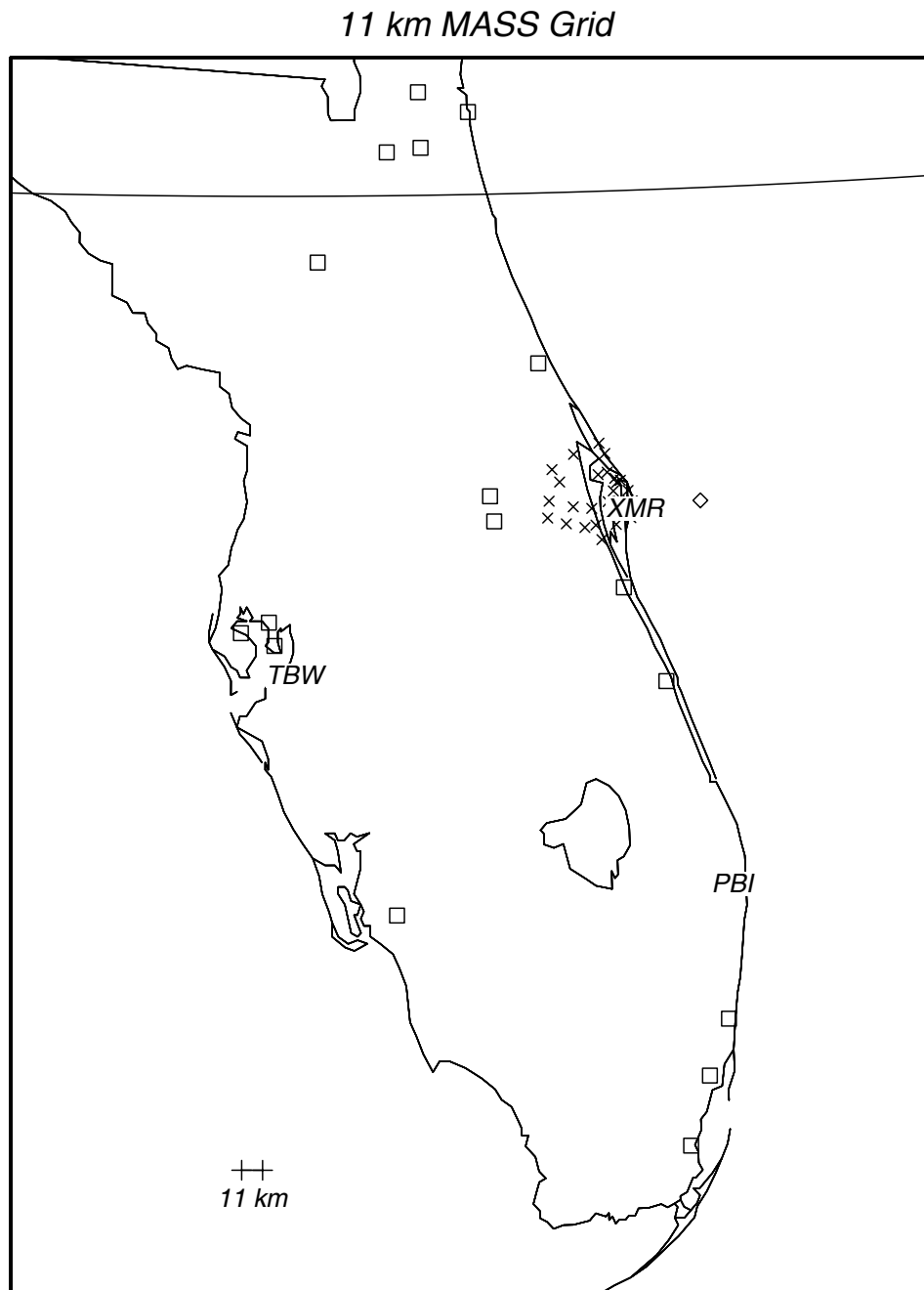
Figure 2.2. Depiction of the geographical domain covered by the horizontal grid matrix used in the 11 km (fine grid) mesoscale simulations. A representative 11 km grid interval is labeled. The locations of available data for typical fine grid model runs are shown as solid dots for rawinsondes, open squares for surface stations, open diamonds for ships and buoys, and 'X's for KSC/CCAS towers. The rawinsonde sites at West Palm Beach (PBI), Tampa Bay (TBW), and Cape Canaveral (XMR) used for verification are indicated by the three letter station identifiers.

2.3 Initiation of Real-Time MASS Runs

The data used to initialize MASS are obtained from the Meteorological Interactive Data Display System (MIDDS) at the Eastern Range. When MASS was delivered to the AMU in March 1993, the system did not contain software to reformat and ingest data from MIDDS. The AMU developed, tested, and implemented routines to reformat MIDDS data and read these data into MASS. In addition, the AMU tested all components of MASS with the new data ingestors, modified and enhanced MESO, Inc.'s UNIX shell scripts to initiate real-time MASS runs, and developed software to view pre-processor and model output using the GEneral Meteorological PAKage (GEMPAK). This software development and testing required the effort of 1 Full Time Equivalent (FTE) for 9 months. During these 9 months, MESO, Inc. provided consulting and additional software at no additional cost that greatly aided the AMU efforts to get MASS running in real-time.

Beginning in January 1994, the AMU began running MASS twice daily on the Stardent 3000 workstation and archiving model output and observations for the model evaluation. The attributes and simulation schedule for the real-time MASS configuration are summarized in Figure 2.3. The daily model forecast and data assimilation schedule consists of two 24-h coarse grid and two 12-h fine grid runs per day. The 24-h coarse grid run designated C00 is initialized with 0000 UTC data and assimilates hourly gridded analyses of surface and MDR data from 0000-0400 UTC. The hourly surface analyses used for data assimilation via Newtonian relaxation or nudging (Table 2.2) are derived from all available synoptic surface, buoy, ship, and KSC/CCAS tower observations at the locations shown in Figures 2.1 and 2.2. The MDR data are transmitted on NCEP's Domestic Data Service at 35 minutes past each hour.   MASS does not presently assimilate any asynoptic data available over the coarse or fine grid domains shown in Figures 2.1 and 2.2. The nudging coefficient is set to 0.0003 for both surface and MDR analysis nudging. Finally, the NGM forecasts generated from 0000 UTC data are used to derive lateral boundary conditions (BC) for the C00 run. The BC are linearly interpolated in time from the NGM forecast data at 0, 6, 12, 18, and 24 h.

The 12-h fine grid run designated F12 is initialized with 1200 UTC data and assimilates 1300 UTC surface and MDR data. The 12-h forecast from C00 (valid at 1200 UTC) provides the first guess fields for the objective analysis of 1200 UTC data used for F12 initialization. Additionally, the 12-24 h forecast fields from C00 are used to specify lateral BC for the F12 run. For each time step of the F12 run, the BC are linearly interpolated from the C00 output at 1-h intervals. The cycle is repeated using 1200 UTC data to initialize the 24-h coarse grid run designated C12 and 0000 UTC data to initialize the 12-h fine grid run designated F00.

The main goal of the daily forecast/assimilation cycle is to initialize the fine grid runs as early as possible with current upper air data. Therefore, the F00 and F12 runs are started approximately 1 h after the synoptic data times of 0000 UTC and 1200 UTC, respectively (Figure 2.3). Since the C00 (C12) forecast is designed primarily to provide first guess fields and lateral BC for the F12 (F00) forecast, it is started well after the synoptic data time at 0715 UTC (1915 UTC). As a result, the 0000 UTC (1200 UTC) NGM initial analyses and forecasts can be used for the C00 (C12) run since all of the 0000 UTC (1200 UTC) NGM gridded data are usually received by 0300 UTC (1500 UTC) at CCAS. The earliest time that forecast products are available and the time that all forecast products are available from coarse and fine grid runs are given in Figure 2.3 It is important to point out these times are for MASS model forecasts executed on an IBM RS 6000/Model 390 rather than the Stardent 3000. The same daily forecast and assimilation cycle shown in Figure 2.3 has been running on the AMU's Model 390 since March 1995. The Model 390 executes MASS approximately three times faster than the four-processor Stardent 3000.

Daily Forecast / Assimilation Schedule

Time (UTC)

| 00 | 06 | 12 | 18 | 00 | 06 | 12 |

04   13 16   01

Coarse grid (45 km)

C00

Fine grid (11 km)

F12

Coarse grid (45 km)

C12

Fine grid (11 km)

F00

▬▬▬ Data Assimilation Mode ——— Forecast Mode | C00 | Cycle Designation

Approximate Daily Job Schedule

| | 00 | 06 | 12 | 18 | 00 |

Time (UTC)

Cycle start time   0105 (F00) 0715 (C00) 1305 (F12) 1915 (C12)

Earliest time forecast products available   0135 (F00)* 0730 (C00)* 1335 (F12)* 1930 (C12)*

Time all forecast products available   0300 (F00)* 0830 (C00)* 1500 (F12)* 2030 (C12)*

*Note product availability times shown are for MASS model runs on an IBM RISC 6000 / Model 390 rather than the Stardent 3000 discussed in the text.

Figure 2.3. Operational real-time daily forecast, data assimilation, and job schedule at KSC/CCAS.

2.4. Statistical Model

The computational constraints and the unavailability of high resolution initialization data prohibit the execution of MASS with sufficient resolution and detailed physics to predict precise occurrences of specific weather phenomena such as thunderstorms and lightning at KSC/CCAS. As a result, a statistical model was incorporated into the MASS prediction system. The basic concept was to combine model and observational data in a way that would permit the generation of hourly updates of the probability of specific weather phenomena at KSC/CCAS during specified time windows. The expectation was that model-generated variables would have more predictive skill in the longer lead-time forecasts (i.e. early in the day) and that the "latest" values of observation-based variables would provide most of the information for the short lead-time (a few hours before the target time window) forecasts. The system was intended to provide a mechanism to transition smoothly from predictions based more heavily on model-generated variables to those based on observational data as the time of the forecast target window approached. This approach is similar in concept to the Model Output Statistics (MOS) schemes used by NCEP to generate forecasts of local variables from regional or global model output.

The statistical model consists of a set of linear discriminant functions (LDFs; Fischer 1938). In the prototype version of the system, LDFs were developed for four consecutive 2-hour forecast time windows covering the period from 1500 UTC to 2300 UTC and four predictand events: (1) a lightning stroke detected within 10 km of the KSC/CCAS weather observation site (TTS); (2) a report of thunder heard at TTS; (3) a report of rain at the TTS site in either regular or special observations; and (4) a report of a wind gust of 15 ms^{-1} or higher at any of the KSC/CCAS mesonet towers within 10 km of TTS. This statistical model can be used to generate an estimate of the probability of the occurrence of each event within any of the forecast windows.

The statistical model was designed to use both observation-based data and model-generated data simultaneously; generate a new forecast each hour; and generate forecasts beginning at 0000 UTC each day for the afternoon period (1500-2300 UTC) of that day. A separate LDF was constructed for each forecast-generation hour for each of the predictands. All of the selected variables (observation-based or model-generated) that were normally available by the start of a particular hour were used as candidate predictors for that hour. Thus, variables based solely on observational data could be included in the prediction equation for any hour after the time that they were reported. For example, a variable based on the MDR data reported at 2035 UTC could be used 25 minutes after the reporting time as a predictor in the 2100 UTC forecast equation. In the case of variables computed from model-generated data, the variables were eligible for consideration as a LDF predictor for any hour after the time that the model simulation normally terminated. Thus, if a scheduled model simulation normally began execution at 0230 UTC and finished at 0630 UTC then any variable computed from the output of that simulation was considered as a candidate only for the LDFs at or after 0700 UTC.

A list of the observation-based and model-generated variables considered as candidate predictors is given in Table 2.3. The predictors for each hour's LDF were selected from the pool of potential predictors by evaluating the discriminating power of all combinations of three variables and selecting the set of three that yielded that highest ability to discriminate between the occurrence and non-occurrence of each event. The predictor set for each hour was limited to three to avoid overfitting of the data in the limited size developmental sample.

Table 2.3.   Observed and forecast predictors for MASS Model Output Statistics

	Observed Predictors
RD500	Distance to closest Manually Digitized Radar (MDR) echo box within 500 km
RD500T	Change in distance to closest MDR echo box
R_500	Number of MDR echo boxes within 500 km
R_500T	Change in number of MDR echo boxes per hour
R_250	Number of MDR echo boxes within 250 km
R_250T	Change in number of MDR echo boxes per hour
VIPDIS	Distance to the nearest level 3 or higher echo
DELVIP	Change in distance to variable VIPDIS per hour
DELDEG	850 mb wind direction minus VIP level 3 cell or higher direction
KSCT	Temperature at TTS or closest available tower
KSCDP	Dew point at TTS or closest available tower
KSCWS	Wind speed at TTS or closest available tower
KSCWD	Wind direction at TTS or closest available tower
KSCU	U wind component at TTS or closest available tower
KSCV	V wind component at TTS or closest available tower
KSCBY	Buoyancy index at TTS or closest available tower
BYTEN	Change in the buoyancy index per hour
RIDGLOC	Location of the ridge axis based on Florida station pressure analysis
ACONV	Convergence x 10^{-5} derived from KSC/CCAS mesonet towers
ACONVT	One hour change in ACONV
NP1	Climatology-based thunderstorm probability from Neumann-Pfeffer
NP2	850 mb wind-based thunderstorm probability from Neumann-Pfeffer
NP3	500 mb wind-based thunderstorm probability from Neumann-Pfeffer
NP4	Stability index-based thunderstorm probability from Neumann-Pfeffer
NP5	800-600 mb mean RH-based thunderstorm probability from Neumann-Pfeffer
KSCLI	Composite lifted index based on KSC sounding
RH500	Surface to 500 mb mean relative humidity from KSC sounding
RH800	800-600 mb mean relative humidity from KSC sounding
DP800	Layer depth where RH >60% from 800 to 600 mb from KSC sounding
DP500	Layer depth where RH >60% from surface to 500 mb
UAVMOI	Average u-wind component where RH >60% from 50 MHz profiler
VAVMOI	Average v-wind component where RH >60% from 50 MHz profiler
ASHEAR	Average shear in all layers from 50 MHz profiler
DIR850	850 mb wind direction from latest KSC sounding
SPD850	850 mb wind speed from latest KSC sounding
LTGDS	Distance to nearest lightning strike from LLP data in first 30 minutes
LTGDST	30 minute change in LTGDS
LTG	Total number of strikes within 60 minutes from LLP data
LTGT	30-minute change in LTG
U850	850 mb u-wind component from latest KSC sounding
V850	850 mb v-wind component from latest KSC sounding
	Mesoscale Atmospheric Simulation System (MASS) Model Predictors
rCAPEn	Convective Available Potential Energy (CAPE) at point nearest TTS
rU850n	850 mb u-wind component at grid point nearest TTS
rV850n	850 mb v-wind component at grid point nearest TTS
rV700n	700 mb vertical velocity (μbars s^{-1}) at grid point nearest TTS
rRELHn	800-600 mb mean relative humidity at grid point nearest TTS
rQCONn	Maximum sigma layer-1 moist convergence index within 100 km of TTS
rPRECn	Convective precipitation over 4 model grid points closest to TTS
rDISTn	Nearest distance from TTS to model grid point with precipitation

r stands for run: C=Coarse grid (45 km) 0000 UTC run (completed by 1000 UTC)
                          F=Fine grid (11 km) 1200 UTC run (completed by 1500 UTC)

n stands for averaging period: 1=1500-1700 UTC
                                              2=1700-1900 UTC
                                              3=1900-2100 UTC
                                              4=2100-2300 UTC

 Example: CCAPE3 = CAPE averaged over hours 1900-2100 from the Coarse grid run

A preliminary set of LDFs were derived from a sample of 58 warm season cases from the summer of 1992. The 58 cases were a subset of a sample of 102 cases for which real-time MASS simulations were generated on a daily basis between mid-July and October of 1992. The sample size for the derivation of the statistical equations was set to 58 because that was the number of cases for which a complete set of observational and simulated data needed to define the predictors and predictands was available. The dominant reason that cases in the 102-case database of real-time MASS simulations had to be excluded from the statistical sample was the inability to retrieve data from KSC/CCAS sensors because of communications difficulties. As a result, the sample size was undesirably small. The small sample size prevented MESO, Inc. from evaluating the statistical equations on an independent data set.

2.5 MASS Evaluation Protocol

In March 1994, the AMU distributed a document presenting a plan for evaluating the MASS model. The AMU solicited comments, questions, and concerns from the Range Weather Operations (RWO), Spaceflight Meteorology Group (SMG), and National Weather Service (NWS) Melbourne (MLB). RWO, SMG, and NWS MLB concurred with the AMU's recommended strategy for evaluating the model. The following sections present highlights of this evaluation protocol.

2.5.1   Objective Evaluation Strategy

The objective verification of the MASS model included gridded and point (or station) comparisons of predicted and observed variables. The coarse and fine grid MASS analyses were generated every 12-h. First guess fields for the coarse grid objective analyses and boundary conditions were derived from Nested Grid Model (NGM) output. Similarly, first guess fields for the fine grid objective analyses and boundary conditions were derived from coarse grid output. Therefore, coarse grid forecasts were highly dependent on NGM forecast errors and fine grid forecasts were highly dependent on coarse grid forecast errors. For these reasons, it is important to quantify and compare coarse grid and NGM forecast errors. Tables 2.4, 2.5, and 2.6 summarize the key aspects of the objective evaluation criteria.

2.5.1.1   45 km (Coarse) Gridded Verification

The 12-h and 24-h coarse grid MASS model forecasts were compared with the corresponding MASS analyses over the entire coarse grid domain. Additionally, the 12-h and 24-h NGM forecasts were compared with the corresponding NGM analyses over the same domain. For grid point comparisons, standard statistics such as RMSE and bias were used to verify temperature (°C), relative humidity (%), and wind speed (m s^{-1}) at 850 mb, 500 mb, and 300 mb, temperature, dew point temperature, and vector wind at 10 m, and mean sea-level pressure (MSLP).

The verification of MASS model precipitation forecasts required observed data that can accurately sample the highly variable spatial and temporal patterns of precipitation. The MASS model precipitation forecasts were verified using hourly rain gauge observations collected by KSC/CCAS and the Florida water management districts over the entire state (excluding the panhandle). These data were available in digital form approximately two months after the observations were collected.

Table 2.4.   NGM objective evaluation criteria

	Variable	Level	Forecast Time	Verification Data
Gridded	T, RH[1], u, v	850, 500, 300 mb	12-h, 24-h	NGM analyses

[1]RH = relative humidity (RH)

Table 2.5.   45 km coarse grid objective evaluation criteria

	Variable	Level	Forecast Time	Verification Data
Gridded	T, RH[1], u, v	850, 500, 300 mb	12-h, 24-h	MASS analyses
	T, T_d[2], u, v	10 m	12-h, 24-h	MASS analyses
	MSLP[3]	--	12-h, 24-h	MASS analyses
	precipitation	surface	hourly	rain gauge analyses
Station	T, T_d, u, v	mandatory levels	12-h, 24-h	rawinsondes
	u, v	2 km, 3 km, etc.	hourly	KSC wind profiler
	T, T_d, u, v, MSLP	surface	hourly	surface stations
	precipitation	surface	hourly	rain gauges
	T, u, v	54 ft	hourly	KSC towers

[1]RH = relative humidity (%)

[2]T_d = dew point temperature

[3]MSLP = mean sea level pressure

Table 2.6.   11 km fine grid objective evaluation criteria

	Variable	Level	Forecast Time	Verification Data
Gridded	precipitation	surface	hourly	rain gauge analyses
Station	T, T_d[1], u, v	mandatory levels	12-h	rawinsondes
	u, v	2 km, 3 km, etc.	hourly	KSC wind profiler
	T, T_d, u, v, MSLP[2]	surface	hourly	surface stations
	precipitation	surface	hourly	rain gauges
	T, u, v	54 ft	hourly	KSC towers

[1]T_d = dew point temperature

[2]MSLP = mean sea level pressure

2.5.1.2   11 km (Fine) Gridded Verification

The 12-h gridded forecasts from the 11 km fine grid MASS model runs were not verified against the corresponding 11 km MASS analyses at or above the surface. The 11 km gridded statistics were not computed because, at this resolution, the model generated features such as mesolows and mesohighs associated with areas of convection that were often be poorly resolved or not resolved by the analysis of surface and rawinsonde observations.

However, 11 km gridded precipitation forecasts were verified using the high spatial and temporal resolution rain gauge data. The rain gauge data were objectively analyzed to the model's fine grid over the Florida peninsula for comparison with the 11 km gridded precipitation forecasts. The statistics and procedures used to verify fine grid precipitation are presented in Section 3.

2.5.1.3   Station Verification

The skill of coarse and fine grid temperature, moisture, and wind forecasts at individual stations or points was assessed by interpolating the model data to the observation locations and then computing statistics such as RMSE and bias. The coarse (45 km) and fine (11 km) grid forecast output was compared with temperature, dew point temperature, and wind at mandatory levels from 0000 UTC and 1200 UTC rawinsondes, 50 MHz profiler winds at specified heights (2 km, 3 km, etc.), hourly temperature, dew point temperature, wind, and MSLP from surface stations, hourly precipitation, and hourly temperature and wind at the 16.6 m level from KSC/CCAS instrumented towers.

The comparisons of model forecasts with station observations were restricted to land grid points only within a subset of the 11 km domain since, with the exception of precipitation data, mesoscale data are available primarily around KSC/CCAS. Additionally, the comparison of 45 km and 11 km grid forecasts at the same location was only possible during the 12-h fine grid forecast period over the smaller fine grid domain. However, point forecasts were evaluated using coarse grid output from the 12-24 h period of the coarse grid runs.

2.5.2   Subjective Verification

The subjective or phenomenological verification of the MASS model planned to use a case study approach to document the success and failure of model forecasts during specific weather regimes. Individual forecasts were to be examined to reveal aspects of model performance in different regimes which are masked by compositing error statistics over many cases. In addition, sensitivity experiments were to be performed on the selected cases to isolate how and why various attributes of MASS (such as initial or assimilated data, physics, resolution, etc.) affect model forecast skill.

2.5.3   Model Output Statistics (MOS) Verification

The observational and forecast data from the 45 km and 11 km simulations during 1992 were used by MESO, Inc. for the derivation of the MOS equations. Given the small sample size, there was no attempt to isolate the relative impact of any data subset (e.g. only 11 km forecasts and observations) on the discriminating power of the LDFs. The AMU compiled simulated and observational data from daily real-time MASS runs during the warm seasons of 1994 and 1995. This database permitted the statistical equations to be derived from a larger sample size and also

provided an opportunity to evaluate the statistical models on an independent data sample. The results of the AMU rederivation and evaluation of MOS are discussed in Section 3.

3.0   Results of MASS Evaluation

This section presents the results of the MASS evaluation including real-time run statistics, objective verification, MOS verification, and the evaluation of real-time MASS output by forecasters and meteorologists at RWO, SMG, and NWS MLB.

3.1 MASS Real-Time Run Statistics

The AMU archived real-time all available coarse and fine grid forecasts and observations for a 9 month period from 15 January 1994 through 15 October for model verification. The AMU continued to run MASS in real-time after 15 October 1994 so that model initialization and forecast products could be transferred back to MIDDS for examination by RWO, SMG, and NWS MLB forecasters and meteorologists. In addition, the model runs were still being archived so that MOS could be generated from the largest possible sample of real-time cases during the 1994 and 1995 warm seasons. The MASS runs were discontinued at the end of January 1996 so the AMU now has an archive of forecasts and observations for 1995 and 1996.

At the end of the 9 month archiving period, the number of completed MASS model runs was compared with the number of total possible runs to measure system stability. During this time, no model forecasts were lost due to instabilities generated by the model's physics or dynamics or problems with the model or data pre-processor software. Furthermore, the majority of 45 km runs that were lost were due to hardware problems or loss of NGM data used as first guess fields in the MASS pre-processor. In an operational setting, MASS would likely be configured to run on a redundant system and to use alternate first guess data sets such as Eta gridded data. In that case, none of these 45 km forecasts would have been lost.

From 15 January through 15 October 1994, there were a total of 462 complete 45 km (coarse grid) runs and 440 complete 11 km (fine grid) runs out of a total 548 possible runs. When a coarse grid run failed, the fine grid run was not executed. At times, the coarse grid run could be restarted and executed at the time that the fine grid would normally run. As a result, the number of complete 45 km and 11 km forecasts do not match exactly.

The statistics reveal 10.9% of the coarse runs were lost due to hardware problems, 2.4% due to software problems, and 2.4% due to loss of data. The hardware problems were related to disk and power supply failures while the software problems were related to changing the procedures that handle data processing. The loss of data includes only NGM gridded data that are required as first guess fields in the MASS pre-processor. The statistics also show that of the 462 complete 45 km runs, 425 (92%) used NGM analysis grids valid at the time of model initialization, while 37 (8%) used NGM forecast grids from the previous (12-h old) forecast cycle.

3.2 Objective Evaluation of MASS at Rawinsonde Sites

The analyses and forecast fields from all available coarse grid, fine grid, NGM, and persistence forecasts from 15 January 1994 through 15 October 1994 are bilinearly interpolated to the rawinsonde station locations at West Palm Beach, FL, Tampa Bay, FL, and Cape Canaveral, FL. These sites are selected because they are the only rawinsonde locations contained within the MASS fine grid and coarse grid domains. The NGM and persistence errors are included to provide a benchmark for MASS forecast errors.

The two statistical measures used here to quantify model forecast skill are the bias and RMSE computed from the twice-daily (0000 UTC and 1200 UTC) rawinsonde observations of temperature (˚C), RH (%), and wind speed (m s^{-1}) at 850 mb, 500 mb, and 300 mb. Errors which are greater than two standard deviations from the mean forecast minus observed differences are removed. The errors at each pressure level and forecast time (i.e., 0 h, 12 h, and 24 h) are averaged for all three stations at both 0000 UTC and 1200 UTC verifying times over the entire 9 month period. Therefore, the maximum number of data points (N) used to derive the average bias and RMSE at a given pressure level and time is 1644 (i.e., 548 total possible runs x 3 stations). The actual value of N varies depending on the variable and pressure level and is usually greater than 1000. The persistence forecasts were generated by assuming that observations of temperature, wind, and moisture at a given pressure level and station were constant for the subsequent 12-h or 24-h period.

3.2.1 Temperature Bias and RMSE

The bias and RMSE in temperature (T) are shown in Table 3.1. The coarse and fine grid T bias at 300 mb, 500 mb, and 850 mb are less than 0.1˚C in the initial analyses (Table 3.1). In contrast, the NGM analyses show a negative (cool) bias at all three levels of more than -0.5˚C. By 12 h, the coarse and fine grid runs develop a cool bias at 500 mb and 300 mb on the order of -0.7 to 1.0˚C that is slightly larger than the NGM cool bias at this time (Table 3.1). At 850 mb, MASS runs show a small positive (warm) T bias of less than or equal to 0.4˚C in contrast to the cool bias of -0.8˚C in the NGM runs. The 24-h MASS coarse grid T bias at 500 mb and 300 mb remains negative on the order of -1.0˚C and positive at 850 mb. The persistence forecasts of T at 12 h and 24 h are basically unbiased at all three levels (Table 3.1).

The RMSE in T from coarse and fine grid analyses (0 h) are less than 0.5˚C at 850 mb, 500 mb, and 300 mb. In the 0-h NGM analyses, the RMSE in T are approximately twice as large at all levels compared with those from MASS. At 12 h and 24 h, the RMSE in T from the coarse grid, fine grid, NGM, and persistence forecasts are on the order of 0.9-1.5˚C at all levels. The RMSE in T from MASS forecasts increase most notably between 0 h and 12 h (Table 3.1).

3.2.2 Relative Humidity Bias and RMSE

The RH bias and RMSE in RH are shown in Table 3.2. At 300 mb, MASS coarse and fine grid analyses display a negative (dry) bias of about -8% whereas the NGM analyses show a positive (wet) bias on the order of 6% (Table 3.2). The wet bias at 300 mb persists in the NGM forecasts increasing to more than 20% by 24 h. In contrast, the coarse grid runs do not maintain the initial dry bias (Table 3.2). However, the fine grid runs develop a wet bias of less than 10% at 300 mb in the 12-h forecasts. An initial small dry (negative) bias at 850 mb in MASS coarse analyses increases to nearly -10% by 24 h. As with T, the persistence forecasts of RH at 12 h and 24 h are basically unbiased at all three levels (Table 3.2).

The RMSE in RH from the MASS and NGM analyses (0 h) range from about 8% to 18% at all three pressure levels and show a tendency to increase with decreasing pressure except for fine grid RMSE in RH at 500 mb (Table 3.2). The NGM RMSE in RH exceed 30% and are largest in the 24-h forecasts (Table 3.2). The MASS RMSE in RH are of the same magnitude as those from the NGM at 12 h and 24 h at 850 mb and 500 mb.

Table 3.1.   Bias and Root Mean Square Error (RMSE) in temperature (˚C), at 850 mb, 500 mb, and 300 mb for MASS coarse grid (MASS-C), MASS fine grid (MASS-F), NGM, and persistence (PERSIS) forecasts. Note that persistence errors are computed only at 12 h and 24 h while fine grid forecast errors are computed only at 0 h and 12 h

Forecast Hour	Pressure Level (mb)	Bias in temperature (˚C)			
		MASS-C	MASS-F	NGM	PERSIS
0	300	0.0	0.1	-0.9	--
	500	0.0	0.0	-0.8	--
	850	0.0	0.0	-0.6	--
12	300	-0.7	-1.0	-0.6	0.0
	500	-0.8	-1.0	-0.5	0.0
	850	0.2	0.4	-0.8	0.0
24	300	-1.0	--	-0.6	0.0
	500	-1.1	--	-0.6	0.0
	850	0.2	--	-1.1	0.1
Forecast Hour	Pressure Level (mb)	RMSE in temperature (˚C)			
		MASS-C	MASS-F	NGM	PERSIS
0	300	0.5	0.4	1.2	--
	500	0.5	0.4	1.1	--
	850	0.5	0.4	0.9	--
12	300	1.3	1.4	1.2	1.2
	500	1.2	1.4	1.0	1.1
	850	0.9	1.0	1.2	1.1
24	300	1.5	--	1.2	1.4
	500	1.4	--	1.1	1.4
	850	1.0	--	1.4	1.3

3.2.3   Wind Speed Bias and RMSE

Table 3.3 displays the wind speed bias and RMSE in wind speed. The NGM and MASS analyses exhibit a negative (slow) bias at all three levels that is maintained at 12 h and 24 h (Table 3.3). The largest bias occurs at 500 mb in 12-h and 24-h coarse grid and NGM forecasts with values as large as -2 m s^{-1} (NGM 24-h runs, Table 2.3). The persistence forecasts of wind speed at 12 h and 24 h show a much smaller negative bias compared with the MASS or NGM forecasts at all three pressure levels (Table 3.3). The evolution of RMSE in wind speed is similar to that for T and RH in that the largest error growth occurs between 0 h and 12 h for MASS coarse and fine grid runs. However, the MASS RMSE in wind speed are consistently less than those from persistence especially at 300 mb where 24-h persistence RMSE are nearly 6 m s^{-1} (Table 3.3).

Table 3.2. Bias and Root Mean Square Error (RMSE) in relative humidity (%), at 850 mb, 500 mb, and 300 mb for MASS coarse grid (MASS-C), MASS fine grid (MASS-F), NGM, and persistence (PERSIS) forecasts. Note that persistence errors are computed only at 12 h and 24 h while fine grid forecast errors are computed only at 0 h and 12 h

Forecast Hour	Pressure Level (mb)	Bias in relative humidity (%)			
		MASS-C	MASS-F	NGM	PERSIS
0	300	-7.7	-7.8	5.9	--
	500	-0.5	-2.3	-0.9	--
	850	-1.6	-2.6	-0.8	--
12	300	0.6	6.9	17.1	-0.6
	500	-0.2	3.8	2.0	-0.3
	850	-6.0	-8.0	-5.0	-0.4
24	300	1.6	--	23.2	-0.5
	500	-1.0	--	1.6	1.2
	850	-9.1	--	-7.5	-0.7

Forecast Hour	Pressure Level (mb)	RMSE in relative humidity (%)			
		MASS-C	MASS-F	NGM	PERSIS
0	300	12.8	12.9	18.4	--
	500	12.5	14.2	12.8	--
	850	9.2	10.7	8.4	--
12	300	17.1	19.8	26.5	17.9
	500	19.0	22.0	21.1	22.8
	850	15.7	17.8	14.8	17.1
24	300	17.7	--	30.8	18.8
	500	20.8	--	22.5	26.6
	850	17.7	--	16.6	18.2

3.2.4   Summary of Rawinsonde Verification

The MASS model coarse and fine grid analysis RMSE for temperature and wind speed are typically smaller than those from the NGM indicating that the MASS analysis scheme fits the rawinsonde data more closely. At 12 h and 24 h, the errors in the NGM and MASS forecasts for temperature, relative humidity, and wind speed and direction at 850 mb, 500 mb, and 300 mb are similar in magnitude. Additionally, an examination of the temperature, wind, and moisture bias from the 11 km and 45 km MASS model forecasts at these same rawinsonde sites does not reveal any serious systematic errors. In general, MASS predicts the large-scale features that are sampled by twice-daily rawinsonde observations as well as the NGM. Furthermore, the magnitude of the errors for both the NGM and MASS are close to the rawinsonde temperature and wind speed measurement uncertainty of about 0.6˚ and 3.1 m s^{-1}, respectively (Schwartz and Benjamin 1995). Thus, it would be unrealistic to expect that further substantial improvement in temperature forecasts could be diagnosed with rawinsonde data.   The similarity in the error characteristics of the two models is not surprising since the NGM provides lateral boundary conditions for the coarse grid and the coarse grid provides lateral boundary conditions for fine

grid. Under strong inflow conditions, the information introduced at the lateral boundary of the coarse or fine grid domains can impact the forecasts in a relatively short time period.

Table   3.3. Bias and Root Mean Square Error (RMSE) in wind speed (m s^{-1}), at 850 mb, 500 mb, and 300 mb for MASS coarse grid (MASS-C), MASS fine grid (MASS-F), NGM, and persistence (PERSIS) forecasts. Note that persistence errors are computed only at 12 h and 24 h while fine grid forecast errors are computed only at 0 h and 12 h

Forecast Hour	Pressure Level (mb)	Bias in wind speed (m s^{-1})			
		MASS-C	MASS-F	NGM	PERSIS
0	300	-0.2	-0.4	-1.0	--
	500	-0.2	-0.5	-1.1	--
	850	-0.3	-0.6	-1.0	--
12	300	-0.7	-0.6	0.0	0.1
	500	-1.1	-1.4	-1.3	-0.1
	850	-0.8	-0.8	-1.1	-0.1
24	300	-0.4	--	-0.3	-0.2
	500	-1.4	--	-2.0	-0.2
	850	-1.0	--	-1.4	-0.1
Forecast Hour	Pressure Level (mb)	RMSE in wind speed (m s^{-1})			
		MASS-C	MASS-F	NGM	PERSIS
0	300	1.4	1.7	2.3	--
	500	1.1	1.4	1.9	--
	850	1.0	1.5	1.6	--
12	300	3.3	3.6	3.5	4.5
	500	2.6	2.9	2.9	3.3
	850	2.2	2.3	2.4	2.8
24	300	3.6	--	3.7	5.8
	500	2.9	--	3.2	4.2
	850	2.4	--	2.6	3.4

3.3 Objective Verification of MASS Precipitation

The horizontal grid resolution and physical parameterizations in MASS are likely insufficient to produce highly accurate, point-specific forecasts in time or space of warm-season convective precipitation. However, in order to determine how well MASS predicts precipitation, both the coarse and fine grid precipitation forecasts over the Florida peninsula were verified using hourly precipitation data collected by the rain gauge network from the St. Johns River, Southwest Florida, and South Florida Water Management districts and the gauges distributed around KSC/CCAS. These data were provided to the AMU on floppy disks for the period 15 January 1994 through 15 October 1994 for the specific purpose of evaluating the MASS model's explicit precipitation forecasts.

3.3.1 Methodology

The precipitation data were analyzed to the 11 km and 45 km model grids using a two-pass Barnes objective analysis (OA) scheme and a bit-mask. The bit-mask was set up to prevent the OA scheme from extrapolating precipitation amounts in areas with few or no gauge measurements. An example of the 11 km bit-mask and rain gauge distribution for 0100 UTC 16 July 1994 is shown in Figure 3.1. The average distance between rain gauges is approximately 10 km. Since these data were collected only over the Water Management Districts and KSC/CCAS, the MASS precipitation forecasts were not verified along sections of the Florida coasts or over the Gulf of Mexico and Atlantic Ocean (see Figure 3.1).

The hourly gridded precipitation analyses were summed over 12 h and compared with MASS forecast precipitation fields summed over the same 12-h period. An example of observed and forecast precipitation accumulated for the 12-h period from 1200 UTC 16 July to 0000 UTC 17 July is shown in Figure 3.2. The forecast precipitation was generated by the fine grid run initialized at 1200 UTC 16 July and is displayed only in the area of the bit-mask as given by the shading in Figure 3.1. The MASS model produced precipitation over a larger area than was observed for this 12-h period during 16 July.

The precipitation skill scores were computed from four-cell contingency tables shown in Table 3.4 for five precipitation thresholds of 0.01″, 0.10″, 0.25″, 0.50″ and >1.00″. The contingency tables were filled by comparing observed and forecast precipitation for each threshold at every grid point within the 11 km and 45 km bit-mask for all model runs from January through October 1994. The four skill scores computed for each precipitation threshold are the bias, false alarm rate (FAR), probability of detection (POD), and equitable threat score (ETS). The definitions of bias, FAR, and POD are given in Table 3.4 and follow Schaefer (1990). The bias is greater (less) than unity for systematic overpredictions (underpredictions) at each precipitation threshold. The ETS, as defined by Gandin and Murphy (1992), has a value of unity for perfect forecasts and accounts for the probability of occurrence for each event. As a result, an ETS for rare events is higher than an ETS for common events. Unlike the conventional threat score or critical success index (CSI), the ETS can be negative because the off-diagonal terms in the contingency table (Y and X) are weighted by a factor of -1 (e.g. see definitions of ETS and CSI in Table 3.4).

3.3.2 Results

The ETS, bias, POD, and FAR from all 1200 UTC and 0000 UTC 11 km forecasts for each month and precipitation category from May through September 1994 are shown as bar graphs in Figure 3.3. With the exception of the >0.10″ threshold in May, the ETS are less than 0.2 for all other thresholds and months (Figure 3.3a). The model tends to overpredict (underpredict) the precipitation at the lower (higher) thresholds as indicated by bias scores in Figure 3.3b. The FAR is at or above 0.4 (i.e. 40%) for May through September at all precipitation thresholds and greater than 0.7 (70%) at the 0.50″ and >1.00″ thresholds (Figure 3.3c). The POD is greater than 0.5 (50%) for the lowest threshold of 0.01″ and decreases rapidly to less than 0.1 (10%) at the 0.50″ and 1.00″ thresholds (Figure 3.3d). The high POD at the 0.01″ threshold is not that encouraging because the model overforecasts the precipitation at this threshold as evidenced by the bias scores >1.
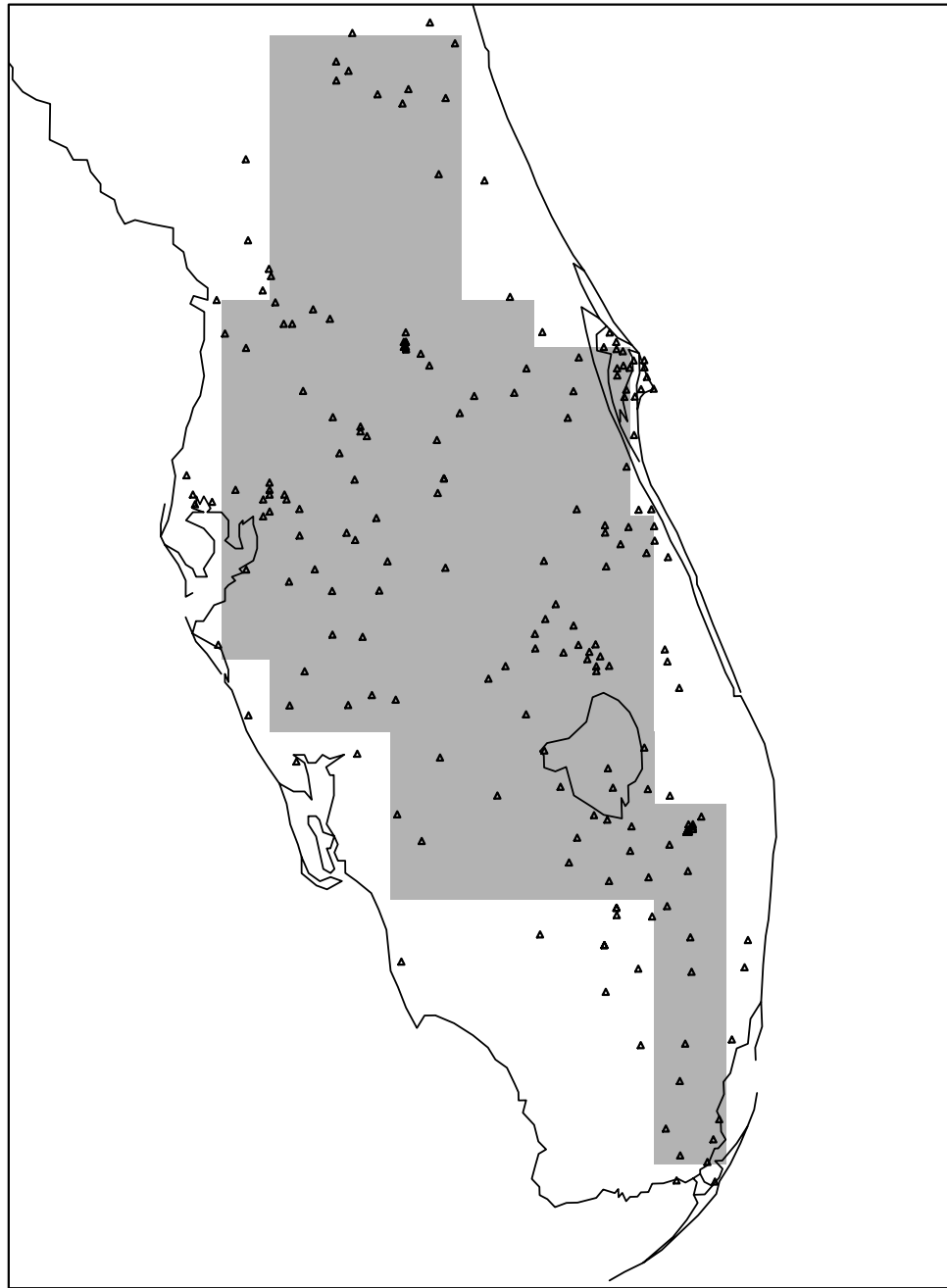
07-16-94 0100 UTC

Figure 3.1. Map depicting the locations of rain gauge observations (triangles) from the St. John's River, Southwest Florida, and South Florida Water Management Districts and the KSC/CCAS region for 16 July 1994 0100 UTC. The gray shading shows the bit-mask for the 11 km MASS grid. The observed precipitation is analyzed to the 11 km model grid only at points contained within the bit-mask.

21

12-h OBSERVED Accum Precip   12-h FORECASTED Accum Precip
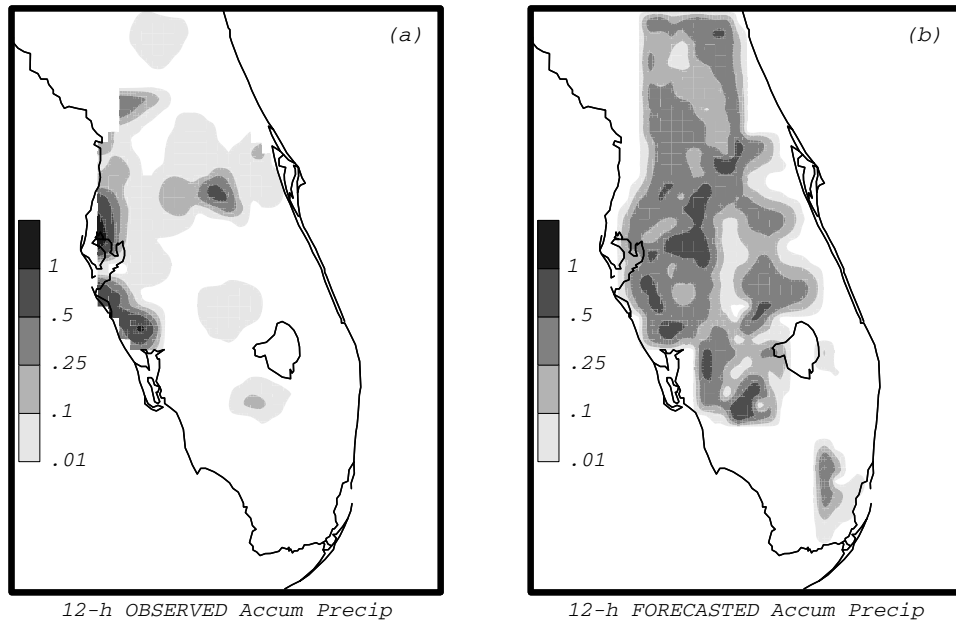
Figure 3.2. Accumulated precipitation (inches) for the 12-h period from 1200 UTC 16 July 1994 to 0000 UTC 17 July 1994. The observed precipitation is shown in panel (a) and the forecasted precipitation is shown in panel (b). The forecasted precipitation was generated by the fine grid run initialized at 1200 UTC 16 July and is displayed only in the area of the bit-mask shown in Figure 3.1. The shading intervals are given by the color bar in each panel for precipitation thresholds of 0.01″, 0.10″, 0.25″, 0.50″, and 1.00″.

Table 3.4.   Example of four-cell contingency table used for gridded precipitation verification

		Observed Precip $\geq$ Threshold	
		Yes	No
Forecast Precip $\geq$	Yes	W	X
Threshold	No	Y	Z

$$\text{bias} = (W + X) / (W + Y)$$

$$\text{false alarm rate (FAR)} = X / (W + X)$$

$$\text{probability of detection (POD)} = W / (W + Y)$$

$$\textit{equitable threshold score (ETS)} = (c_{11}W + c_{22}Z + c_{12}X + c_{21}Y)/(W + X + Y + Z)$$

$$c_{11} = (1-P)/P; \quad c_{22} = P/(1-P); \quad c_{21} = c_{12} = -1$$

$$P = (W+Y)/(W+X+Y+Z)$$

22

Figure 3.3. Objective skill scores from all 1200 UTC and 0000 UTC 11 km from May through September 1994 for precipitation thresholds of 0.01″, 0.10″, 0.25″, 0.50″, and 1.00″.

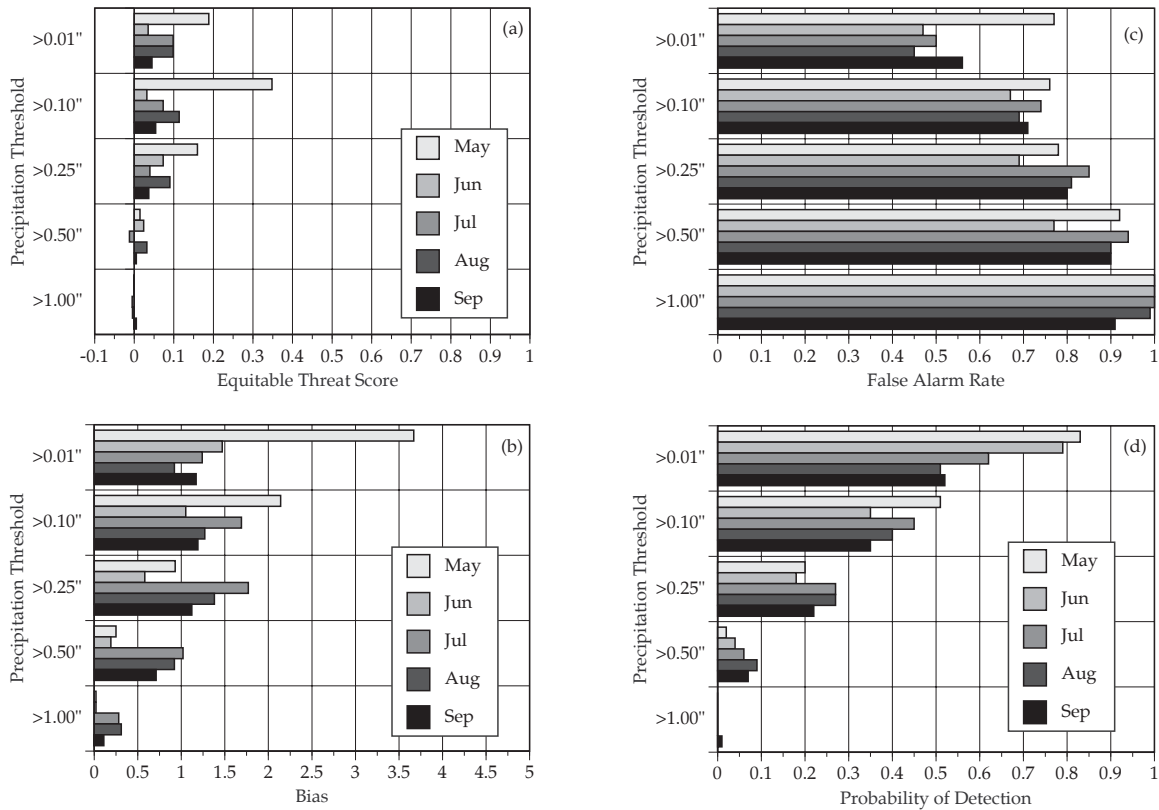The skill scores shown in Figure 3.3 indicate that the fine grid (11 km) MASS runs show little objective skill in predicting the exact location and amount of precipitation during May through September 1994. However, the 11 km runs from January through May 1994 yield higher ETS at the 0.01″ and 0.10″ thresholds (not shown). These results suggest that the MASS model provides more accurate explicit precipitation forecasts when synoptic-scale weather systems and non-convective precipitation dominate the weather in Florida. It is well known that operational models such as NCEP's NGM also show less skill in forecasting warm season precipitation associated with small scale convective-type weather systems.

The ETS from 11 km MASS runs are very similar to those published for operational models such as the NGM and Eta model (Junker et al. 1989; Zupanski and Mesinger 1995). However, it is important to point out that the skill scores such as the ETS do not account for the spatial or temporal errors in precipitation forecasts (Olson et al. 1995). For example, the model may predict the correct amount of precipitation 2 h later and one grid point farther west than observed. In this case, the ETS score would indicate little or no skill in predicting the event, whereas the actual utility of the forecast may be quite good considering the spatial and temporal displacement of forecast precipitation. The AMU examined maps of analyzed and forecast precipitation accumulated for 3-h periods from all 1200 UTC 11 km forecasts during July 1994. This qualitative analysis revealed that the MASS model did not routinely produce the correct distribution of precipitation at any time in the forecast period over any area of the domain.

Based on the ETS derived from mesoscale precipitation data for MASS model runs, it is apparent that precipitation forecasting remains a problem for mesoscale models especially in a sub-tropical environment characterized by weak large-scale forcing such as Florida in the warm season. The fact that the 11 km MASS runs do not show more skill than operational models in forecasting warm season precipitation is likely due to a number of factors including insufficient horizontal resolution and deficiencies in the physical parameterizations, especially the Kuo-Anthes convective scheme. In addition, the components of the surface energy budget such as evapotranspiration and the representation of the existence and impact of sub-grid scale clouds are simplified so that MASS can run in real-time on workstations. Finally, it is difficult to specify accurate mesoscale distributions of atmospheric moisture (including clouds and pre-existing convection), temperature, winds, and moisture in the soil and surface cover layer from the data sources currently used in MASS. The data available from the WSR-88D radars, Doppler wind profilers, the new series of geostationary satellites (GOES-I, J), and Global Positioning System (GPS) satellites may offer an opportunity to improve initialization and short-range forecasts by MASS if they can be incorporated into the system in real-time.

3.4 Rederivation and Evaluation of MASS MOS

The fact that MASS precipitation forecasts even on the 11 km grid are not superior to those from operational models is not surprising since MASS was not designed to provide accurate, explicit forecasts of convective precipitation. Instead, MESO, Inc. combined dynamical model output from MASS with observations to produce probability forecasts for the occurrence of precipitation, thunder, lightning and high winds as described in Section 2.4. These model output statistics or MOS were designed to account for deficiencies in the MASS model.

The AMU evaluated the MOS coefficients derived by MESO, Inc. from their limited sample of 1992 warm season cases. In addition, the AMU rederived and validated MOS using the more complete data base of 1994 and 1995 warm season cases. The rederivation and evaluation of MOS was delayed until the AMU received the software used by MESO, Inc. to derive the original coefficients. MESO, Inc. sent this software to the AMU in January 1995. Since the MOS software used the same data as the MASS model, the AMU had to modify the data ingestors to read observational data in MIDDS format and model data in GEMPAK format.

The coefficients were derived from the 1994 data and verified using 1994 data and independent data from 1995. The coefficients verified using 1994 data showed a severe bias toward over prediction (i.e. an event was forecast to occur far more often than was observed). The bias toward over prediction was not related to any errors in the software. In fact, a similar bias was discovered when the same verification procedure is applied to the coefficients derived by MESO, Inc. using 1992 data. The bias was likely caused by the choice of predictors (Table 2.3), the observed and/or model data used to compute the predictors, and the narrow space-time windows defined for the predictands. As an example, the predictors based on MDR and lightning data were used to define existing areas of convection and changes in the intensity convection. However, these predictors did not account for direction of motion. If the intensity of thunderstorms near TTS were observed to increase for a given hour, but the cells were located to the northeast of TTS and moving south, their impact on subsequent thunderstorm forecasts at TTS would be different than if the cells were initially to the north of TTS and moving south.

In its current form, MASS MOS is not suitable for use as a forecasting tool. The technique could be improved by using NEXRAD rather than MDR data rather to define existing areas of convection, choosing different predictors from both model and observations, and obtaining a complete data set that covers at least five warm seasons.

3.5 Remaining Components of the MASS Evaluation

This sub-section highlights results from the remaining components of the MASS objective verification (Tables 2.4-2.6) and subjective verification that are not been presented in previous sections.

3.5.1   MASS Gridded Verification

As described in Section 2.5.1.1, the 12-h and 24-h coarse grid MASS forecasts were verified and compared with 12-h and 24-h NGM forecasts at 850 mb, 500 mb, and 300 mb. The results (not shown) are very similar to those presented for the rawindsonde (station or point) verification. As with the rawinsonde statistics, this result is expected since the NGM provides lateral boundary conditions for the coarse grid runs. The bias and RMSE statistics for 10 m wind, temperature and moisture at 10 m, and MSLP from MASS were computed from all available 45 km coarse grid runs. However, 10 m and MSLP gridded data from the NGM were not archived so the MASS forecasts of these parameters could not be benchmarked against the NGM. Even if these NGM grids were archived, differences between the methods used to obtain MSLP and 10 m variables in the NGM and MASS could produce errors as large as those due to differences in model physics, resolution, initialization, etc. For these reasons, the results from the MASS gridded verification of 10 m variables and MSLP are not shown.

3.5.2   MASS Station Verification

The coarse (45 km) and fine grid (11 km) MASS wind components were verified using KSC's 50 MHz Doppler Radar Wind Profiler (DRWP) hourly wind profiles at heights of 2-15 km above ground level. The bias and RMSE in wind speed and wind direction were computed at 1 km intervals from 2-15 km and averaged for all MASS runs from January through October 1994 at each forecast hour. The use of the DRWP winds rather than rawindsonde winds allowed the bias and RMSE to be calculated hourly rather than twice-daily (i.e. at the synoptic times of 0000 UTC and 1200 UTC). Despite the higher temporal resolution of DRWP data, the statistics (not shown) do not provide much more information on wind errors than those derived using winds from the XMR rawinsonde site. It is likely that 50 MHz DRWP data would be more useful for diagnosing and verifying individual MASS forecasts and for case studies where significant mesoscale variability in winds above 2 km could not be measured by rawinsondes (Spencer et al. 1996).

The MASS model surface forecasts of temperature, moisture, winds, and pressure were verified against hourly surface airway observations (SAO). In addition, model forecasts of maximum and minimum temperatures from 45 km and 11 km runs were compared with SAO's and benchmarked against persistence and climatology forecasts. The USAF Technical Application's Center (ETAC) provided the data used to generate the climatological forecasts. The MASS forecasts were not verified against other NCEP models such as the NGM because the surface point forecast data from NCEP models were not archived. Finally, the hourly winds at the 54 ft level from the KSC/CCAS instrumented towers were used to verify the MASS forecasts of winds interpolated to the tower locations.

As part of the surface station verification, plots of observed and forecast temperature were examined at several Florida stations including West Palm Beach (PBI), Florida. The time series of forecast temperature at PBI (not shown) revealed a diurnal cycle that was notably damped in comparison with the observed diurnal cycle for the entire month of July 1994. This problem showed up as a negative (cool) bias in temperature that was caused by interpolating the model output to the exact observation location. In the case of the 45 km grid runs (and to a lesser extent in the 11 km runs), the PBI station location is more representative of a water rather than land grid

point. In fact, the temperature trace of the land grid point closest to PBI (not shown) had a much more realistic diurnal cycle.

Another related problem with surface station verification was that model variables should be compared with SAO at the instrument height of 10 m for winds, 2 m for temperature and moisture, and 54 ft for KSC/CCAS towers. The MASS model forecast variables were reduced to these levels using linear interpolation between the lowest model levels and/or the surface. However, this procedure was not consistent with the typical logarithmic profiles of temperature, wind, and moisture observed in the planetary boundary layer (PBL) and treated by the MASS model's PBL parameterization. Due to the problems with vertical interpolation and the representativeness of land versus water grid points at stations near the coast (e.g. TTS; Melbourne, MLB; Patrick Air Force Base, COF; etc.), the results of the MASS station verification at SAO and tower sites are not presented or interpreted. Ideally, the PBL parameterization should output wind at 10 m (54 ft or 16.6 m for KSC/CCAS towers) and temperature/moisture at 2 m so that no additional vertical interpolation is required. In fact, MESO, Inc. modified the PBL scheme in the newer versions of the MASS model to produce gridded fields of temperature and moisture at 2 m.

In general, station verification provides a stringent test of model capabilities since statistics computed for many grid points do not assess model forecast skill at individual locations. However, station observations sample many scales of atmospheric phenomena some of which can not be resolved by the model. Although point verification should benefit higher resolution models which resolve finer scales of motion, it does tend to give a more pessimistic view of model performance than gridded verification. As a result, the verification of MASS model precipitation interpolated to rain gauge locations (i.e. station verification) was not performed since the gridded ETS from MASS were no better than those from operational models such as the NGM.

3.5.3   MASS Case Studies and Sensitivity Experiments

MESO, Inc. provided a detailed analysis of two cases and an overview of five cases from the sample of 102 real-time MASS runs that were performed during the development of the system in 1992. This subjective verification of MASS using these seven cases in presented in MESO, Inc.'s SBIR Phase II final report to NASA that was delivered in March 1993. One of these cases from 19 February 1992 provides an illustration of the improved forecast guidance that could potentially be gained by executing a mesoscale model over the Florida peninsula. This case was important from an operational perspective because the USAF scrubbed the second launch attempt of a Delta II rocket from Launch Complex 17B at CCAS due to thick clouds (> 4500 ft thick) and disturbed weather (i.e. any meteorological phenomena producing moderate or greater precipitation). The adverse weather was related to an area of thunderstorms that developed to the southwest of KSC/CCAS during the afternoon hours in advance of a dissipating frontal band. The forecasters at CCAS set the overall probability of weather constraint violation for the operation to 30% just 90 minutes (2029 UTC) prior to the beginning of the launch window.

The initial development of this isolated convection was not predicted by the NGM but was simulated by the MASS model. The performance of MASS for this case was not spectacular, but it demonstrated the skill that the model can exhibit when mesoscale circulations are an important contributor to the initiation and evolution of convective storms. The discussion and figures for the 19 February 1992 case are not included here since they appear in MESO, Inc.'s final report, in the AMU Quarterly Update Report for the Fourth Quarter FY-95, and in a paper co-authored by Drs. John Manobianco (AMU), Gregory Taylor (AMU), and John Zack (MESO, Inc.) that has been published in the *Bulletin of the American Meteorological Society* (Manobianco et al. 1996).

The example from 19 February 1992 illustrates a case in which the development of moist convection was the result of well-defined mesoscale features that were attributable to differential boundary layer heating. MASS tends to perform well in this type of scenario since (1) many of the factors which control the differential boundary layer heating (land/water distribution, density of vegetation, soil moisture and cloud patterns) can be reasonably well mapped for initialization; and (2) the heating patterns themselves, with the possible exception of those due to cloud shading, do not drastically change during the course of the simulation. In contrast, the model does not perform as well in cases in which the evolution of convection is strongly controlled by the feedback from the convection itself (e.g. the development of new convection along thunderstorm outflow boundaries).

The AMU processed observations and MASS model forecasts for three cases from the 1994-1995 archive including 13 July 1994 (sea breeze), 28 July 1994 (no sea breeze), and 20 May 1995 (Atlas-Centaur launch with GOES-J payload). Although the Atlas-Centaur mission scrubbed due to anvil clouds that were forecasted by the Launch Weather Officer (LWO), there was a 37 kt wind gust measured by the 90-foot tower on the pad at Complex 36B around 0525 UTC prior to the beginning of the launch window. The real-time 0000 UTC 11 km MASS model forecast, available just prior to tower rollback at 0242 UTC, predicted an outflow boundary originating from thunderstorms to the west-southwest of KSC/CCAS. In association with the simulated outflow boundary, MASS forecasted a gust front with sustained wind speeds on the order of 25 kt to move east across Complex 36B around 0300 UTC.

The AMU planned to analyze the 20 May 1995 case to determine if MASS output may have provided value-added to the LWO's forecast for the potential of winds in excess of 22 kt despite the fact that the model missed the timing of the event by nearly two hours. In addition, sensitivity experiments and preliminary analyses of the two warm season cases from 13 July and 28 July 1994 were performed. The sensitivity experiments focused on the impact of initializing soil moisture using antecedent precipitation observations, initializing soil temperature using surface temperature observations, and initializing the 11 km runs with first guess fields from 45 km MASS analyses rather than 12-h, 45 km MASS forecasts. The precipitation skill scores (ETS) from all sensitivity experiments did not show significant improvement over the real-time runs for the two July 1994 cases. However, a more thorough examination of the results is required to determine if other parameters such as surface temperature and wind are sensitive to the initialization of soil moisture and soil temperature and the use of MASS analyses rather than forecasts as first guess fields.

A detailed analysis and discussion of the 20 May 1995 and July 1994 cases was not completed in order to focus efforts on evaluating MOS and on getting real-time MASS output and MOS into MIDDS for examination by RWO, SMG, and NWS MLB (Section 3.6).

3.6 Subjective Evaluation of MASS by RWO, SMG, and NWS MLB

In September 1994, the AMU began running software to provide MASS model initialization and forecast output to the MIDDS. The grids were transferred from the AMU's IBM PC to designated areas on the IBM test machine every six hours. The automated jobs which controlled the transfer process were not executed until the MASS forecasts expired so that the initialization and forecast products could not be used for operational decisions. The purpose in providing MASS output was to solicit feedback from RWO, SMG, and NWS MLB regarding whether MASS provided added value compared with operational models such as the NGM for the analysis and forecasting of weather at KSC/CCAS and surrounding areas.

Mesoscale Atmospheric Simulation System (MASS) Evaluation Worksheet

1. Date: _____ Meteorologist: _____(NWS/RWO/SMG ; Circle one)

2. Mark 'x' for MASS product(s) viewed:

	45 km Coarse Grid (0-24 h fcst)		11 km Fine Grid (0-12 h fcst)	
Product	1200 UTC	0000 UTC	0000 UTC	1200 UTC
Skew-T's				
Time Series				
4-Panel Progs				
2-Panel Progs				
Cross Sections				

	Table of Probabilities
Model Output Statistics (MOS)	

3. Log any problems/concerns with MASS products (e.g. accuracy, availability, format, timelines, etc.):
    _____
    _____
    _____
    _____
    _____

4. Does MASS provide value-added in analysis/forecasting (A/F) of following weather events/parameters**?**

Event	**Value-Added (YES or NO)**	If YES: How was MASS used to aid A/F If NO: Why was MASS unable to aid A/F	Verification Method
Sea-breeze Onset			
Temp. (specify levels):			
Winds (specify levels):			
Moisture (specify levels):			
Stability indices (specify):			
Precipitation /Thunderstorms			
Lightning			
Wind Gusts			
Other (specify):			

5. General Comments/Suggestions:
    _____
    _____
    _____
    _____
    _____

Figure 3.4. Sample worksheet used by RWO, SMG, and NWS MLB for their subjective evaluation of MASS.

The preliminary feedback indicated that forecasters and meteorologists at RWO, SMG, and NWS MLB did not have time to look at expired model products within the context of their normal operational duties. As a result of this feedback and a consensus reached at the April 1995 AMU Tasking Meeting, the AMU started sending real-time MASS output to MIDDS beginning in April 1995. In addition, the AMU was asked to develop a MASS evaluation worksheet that would help RWO, SMG, and NWS MLB provide specific feedback to the AMU regarding the utility of MASS forecasts during the 1995 warm season (May-September). An example of this worksheet is shown in Figure 3.4.

The model output was sent to MIDDS as graphical products (horizontal and vertical cross sections, time series, time-height cross sections, and soundings) saved as images and MOS data saved as text bulletins. The graphical image products rather than raw model grids were transferred to MIDDS primarily because the AMU PC Model 80 did not have enough speed to process large data sets (~20-30 MB) that were needed by MIDDS to generate vertical and time-height cross sections.

There were several issues that prevented RWO, SMG, and NWS MLB from accessing and evaluating MASS model output on a regular basis until the end of July 1995. First, there were problems with the transfer of MASS to MIDDS that had the largest impact on NWS MLB who accessed MIDDS via modem. Second, the operational requirements from April to July 1995 associated with the large number of missions at KSC/CCAS and high frequency of tropical storm activity in the Atlantic basin made it difficult for RWO and SMG to spin up on the MASS evaluation. In fact, NWS MLB began evaluating MASS as early as June 1995 while SMG did not start looking at MASS output until the end of August 1995. Despite these problems, the MASS evaluation based on the parameters shown in Figure 3.4 continued until the beginning of October 1995. After that time, RWO, SMG, and NWS MLB summarized their subjective evaluations of MASS in memoranda that were forwarded to the AMU by November 1995.

Overall, RWO stated that MASS would be an asset to routine Eastern Range forecast operations. In addition, NWS MLB indicated that MASS showed reasonable utility and occasional improvement over the NCEP operational regional-scale models. SMG found that MASS was occasionally helpful in generating SMG forecasts, but most times MASS did not improve on data output from other models (Eta, NGM, MRF). SMG also noted several instances where MASS was far off base and could have adversely affected SMG forecasts. However, SMG noted that due to the limited number of days evaluated during the late summer/early fall time frame, SMG's evaluation may not be completely representative of the MASS model's capabilities.

4.0   Summary and Recommendations

This section summarizes the results from the MASS evaluation, highlights the current status of the MASS, and concludes with recommendations for improving local mesoscale modeling systems like MASS and lessons learned from the MASS evaluation.

4.1 Summary of MASS Evaluation

The AMU ran MASS twice-daily on a Stardent 3000 workstation for two years from January 1994 through January 1996 and archived both model output and observations for the purpose of model evaluation. The following sections summarize the key points of the MASS evaluation.

4.1.1   Real-Time Run Statistics

During the 9 month period from 15 January 1994 to 15 October 1994, the largest percentage (10.9%) of missed runs resulted from hardware failures. In an operational setting, MASS would likely run on a redundant system which could have prevented these lost runs. Overall, no model forecasts were lost due to instabilities generated by the model's physics or dynamics or problems with the model or data pre-processor software. This result suggests that MASS is extremely robust and would be a very reliable operational system.

4.1.2   Objective Evaluation at Rawinsonde Sites

An examination of bias and RMSE for temperature, wind, and moisture from MASS versus the NGM at selected rawinsonde stations over all available cases from January through October 1994 reveals that MASS is predicting the large-scale features as well as the NGM. This result is expected since the NGM provides lateral boundary conditions for the 45 km MASS runs. In fact, verification of parameters whose variance is dominated by large-scale processes is unlikely to reveal a large improvement by mesoscale models such as MASS since much of the variance is already accounted for by regional-scale models such as the NGM.

4.1.3   Objective Evaluation of Precipitation

The AMU verified precipitation forecasts from MASS using rain gauge data with roughly 10 km spacing over the Florida peninsula. The ETS derived from 11 km runs for May through September 1994 are less than 0.4 and are not consistently better than those reported for operational models such as the NGM and Eta. However, MASS does show greater skill as evidenced by higher ETS from January through May 1994 (not shown).

4.1.4   Rederivation and Evaluation of MOS

The AMU evaluated the MOS coefficients using MESO, Inc.'s limited data base of 1992 warm season cases and rederived and validated MOS using the complete data base of 1994 and 1995 warm season cases. The coefficients verified using 1992 and 1994 data show a severe bias toward over prediction that is likely caused by the choice of predictors and the observed and/or model data used to compute the predictors. In its present form, MASS MOS is not suitable for use as a forecasting tool.

4.1.5   Remaining Components of Evaluation

The AMU performed gridded verification, selected station verification, case studies, and sensitivity experiments. These verification results are not included in this report for the reasons given in Section 3.5. Nevertheless, the 19 February 1992 case illustrates the utility of running MASS at 11 km over the Florida peninsula when mesoscale circulations are an important contributor to the initiation and evolution of convective storms. The performance of the 11 km MASS run for this case while not spectacular, was superior to the 80 km NGM forecast especially with respect to the distribution of precipitation.

4.1.6   RWO, SMG, and NWS MLB Evaluation of MASS

The RWO, SMG, and NWS MLB examined MASS model output in the form of images and text bulletins (MOS forecasts) for a portion of the 1995 warm season. Each group focused their evaluation on slightly different model products and found that MASS was occasionally more useful than NCEP regional models for short-range (<24 h) forecasting. SMG also noted several instances where MASS was far off base and could have adversely affected SMG forecasts. However, the results of this real-time evaluation by RWO, SMG, and NWS MLB may not be completely representative of the model's capabilities since each group was only able to examine a limited number of cases using a very small fraction of available model output.

4.2 Current MASS Status

At the end of January 1996, a teleconference was convened with NASA Headquarters, NASA KSC (AMU), RWO, SMG, and NWS MLB to review the results of the MASS evaluation and discuss options for a "mid-course correction" to the AMU mesoscale modeling task. A subsequent teleconference with the same parties was convened during the first week of February 1996 to make a decision regarding the "mid-course correction" for the AMU modeling task. Based on consensus from RWO, SMG, and NWS MLB during the February 1996 telecon, the AMU was directed to terminate all work with MASS and write this final report. In addition, the AMU was tasked to prepare plans to continue running the current or upgraded version of MASS on a non-interference, zero-labor cost basis. Finally, the AMU was tasked to begin evaluating NCEP's 29 km Eta model.

The "mid-course correction" to the AMU modeling task was based on consensus that

- The current version of MASS does not provide sufficient added value over NCEP models to justify the cost of continuing the evaluation with the intent to transition MASS for operational use,

- An evaluation of the 29 km Eta model over the next 12 months will likely result in a low-to-medium risk, short-term payoff, namely that the AMU will be able to determine the utility of NCEP's best mesoscale model for local forecasting, and

- The real-time data deficiencies (e.g. limited access to NCEP gridded data and no access to digital NEXRAD and 915 MHz DRWP data) would likely be corrected over the next 12-24 months which may increase the utility of local modeling systems such as MASS if these data can be incorporated into the systems in real-time.

4.3 Recommended Local Mesoscale Modeling Enhancements

In order to make MASS a cost-effective system, the AMU recommends the following changes and improvements.

- Extend the 11 km runs from 12 h to 24 h and expand the 11 km domain from 45x60 to 75x70 grid points and 20 to 30 vertical levels.

- Discontinue twice-daily 24-h 45 km (coarse grid) runs and perform only twice-daily 11 km (fine grid) runs.

- Initialize MASS with 48 km or 29 km Eta rather than 80 km NGM gridded fields.

- Initialize sea surface temperatures (SST) with real-time analyses rather than monthly climatology.

- Install version 5.9.3 of the MASS data pre-preprocessor that contains a new soil texture database, improved vegetation climatology, and a new three-dimensional multivariate optimum interpolation for objective analysis of initial data.

- Install version 5.9.3 of the MASS model that allows larger long-to-short time step ratios which shorten total model run times, and contains improved boundary layer, surface hydrology, and microphysical parameterizations.

- Run MASS on a faster workstation than the 4-processor Stardent 3000.

- Improve the operational communication networks so that local mesoscale model products could be accessed by RWO, SMG, and NWS MLB in a timely, efficient manner.

In their subjective evaluations of MASS, the RWO and NWS MLB indicated that it would be beneficial to extend the 11 km runs from 12 h to 24 h. In fact, SMG inquired about this option after reviewing the AMU's proposed MASS configuration memorandum that was distributed in early 1994. SMG favored this configuration so that 24-h 11 km forecasts initialized at 0000 UTC could provide guidance for Shuttle landings occurring after 1200 UTC when similar 12-h 11 km forecasts would have expired.

In order to execute the 24-h 11 km runs over a larger domain, it would be necessary to discontinue 45 km runs so that the forecasts can be completed in a timely manner. Preliminary tests indicate that 24-h 11 km MASS model products would be available at roughly the same time that 24-h 45 km MASS model products are now available. The horizontal extent of the 11 km domain should be expanded in order to minimize the impact of boundary conditions which have more time to affect the interior solution in longer runs. The boundary conditions for 11 km runs would be provided every 6 h by the 48 km (or 29 km) Eta model rather than every hour by the 45 km model runs.

In order to make substantial improvements in warm season explicit precipitation forecasts, it is likely that deficiencies with respect to model resolution, model physics, and initialization data described in Section 3.3.2 would need to be corrected. Currently, it is difficult to initialize the mesoscale structure of atmospheric moisture, temperature, winds, and moisture in the soil and

surface cover layer from the data sources ingested by MASS. The data available from WSR-88D radars, 915 MHz DRWP, Radio Acoustic Sounding Systems (RASS), satellites (GOES-I, J and GPS), and soil moisture probes may offer the opportunity to improve initialization and short-range forecasts by MASS if they can be incorporated into the system in real-time.   The recommended enhancements to MASS listed at the beginning of this section focus primarily on upgrades to the software and changes to the real-time run configuration. However, these software upgrades and modifications to the configuration do not increase the horizontal resolution of MASS and do not include better initialization data except for Eta grids and real-time SST.

It is important to point out that increasing the resolution of MASS, and using better physical parameterizations and initialization data will not necessarily improve the utility of MASS forecasts to the point where they will always have added value over NCEP models. The primary benefit of running a local mesoscale model is that it can be tailored for specific, forecasting problems. However, local workstation-based, real-time modeling systems must run fast enough so that the forecasts can be used before they expire. This obvious and critical aspect of these systems must be balanced against the desire to improve the quality of the simulations by increasing the resolution, using more sophisticated physical parameterizations and incorporating better mesoscale initialization data. Since the monetary cost of computational power continues to decrease with further advances in microprocessor and parallel processing technology, there is still opportunity for rapid advancement in model performance. Hence, a workstation-based numerical forecast system should be viewed as a dynamic entity and should evolve in tandem with the processing power available at a specified cost.

Another advantage of local modeling is that users can choose the

- Type and frequency of output products,

- Model configuration (the cycle times, grid resolution, model physics, domain size, etc.), and

- Types of local data (e.g. WSR-88D, 915 MHz and 50 MHz profiler, KSC/CCAS tower, etc.) and parameters (e.g. vegetation, land use, soil moisture, etc.) used for model initialization.

Nevertheless, these advantages must be weighed against the life-cycle costs and expertise needed to maintain a local modeling system. The real-time run statistics presented in Section 3.1 indicated that MASS would be a very reliable operational system. However, the current version of MASS delivered on the Stardent 3000 has not been upgraded since March 1993. If MASS were ever transitioned for operational use, the AMU suggests

- Periodic hardware upgrades to take advantage of cheaper, faster workstations that could support finer resolution runs with more sophisticated physical parameterizations over larger domains,

- Periodic software upgrades to take advantage of improvements in the MASS pre-processor and model, and

- Technical system support provided by the vendor to resolve major problems with new or existing versions of MASS.

Finally, there is a problem with the large amount of data generated by local mesoscale models that can not easily be distributed to users in a timely, efficient manner. In fact, the NWS also faces this problem since NCEP generates several gigabytes of model output each day that all Weather Forecast Offices (WFO's) cannot access due to inadequate communication bandwidth. While this deficiency presents a challenge to local modeling at KSC/CCAS, it should not stand in the way of progress on such an effort. The transition plan for a system like MASS should specify requirements for sufficient communication bandwidth to handle the large volume of data produced by a local mesoscale model.

4.4 Lessons Learned from MASS Evaluation

The AMU's work on the installation and evaluation of MASS spanned nearly 3 years from early 1993 through the end of 1995. During that time, the AMU learned a number of valuable lessons about the evaluation, application, and utility of local mesoscale models. These lessons are described briefly in this section so that any future efforts with local modeling can take advantage of this information. To some extent, the design of the 29 km Eta model evaluation will consider these points.

The first five bullets relate to the installation and evaluation of MASS.

- The software routines that handle data pre-processing should be structured to accept local real-time data sets prior to the delivery of a modeling system to KSC/CCAS. To accomplish this task, the vendor would need current, sample data sets (e.g. from MIDDS) so that the system could be tested using the same data stream that would be available locally at KSC/CCAS.

- The evaluation protocol for MASS could have included more benchmarking with existing NCEP models (e.g. NGM, Eta, regional spectral model, Rapid Update Cycle, etc.), other forecast methods (e.g. persistence, climatology, etc.), and other forecast tools (e.g. Neumann-Pfeffer thunderstorm probabilities). The additional benchmarking would help to quantify the added value of a local model and provide information for a cost-benefit analysis that would be required before a decision was made to transition a local modeling system for operational use.

- The evaluation protocol could have included more phenomenological verification and stratified model error based on specific weather regimes. For example, bias and RMSE errors in temperature, winds, and moisture could have been stratified by layer-averaged wind direction. In addition, the verification could have focused more on events such as the sea-breeze.

- The evaluation protocol could have included daily, real-time forecasting by AMU personnel to determine the most effective ways to visualize, interpret and use MASS for short-range forecasting in east central Florida (KSC/CCAS and surrounding areas).

- In general, the evaluation of mesoscale models should use all available mesoscale data sets. However, these data sets can be quite large and require extensive processing and quality control before they can be used for verification. For the evaluation of 11 km MASS runs, the KSC tower and KSC/CCAS and Florida water management rain gauge observations had sufficient horizontal resolution to verify hourly wind and precipitation

forecasts, respectively. Similarly, the 50 MHz DRWP data had sufficient temporal resolution to verify hourly wind profiles above 2 km from either the 45 km or 11 km runs. Future mesoscale model evaluations could use these same data sets in addition to data from the KSC/CCAS 915 MHz boundary layer profilers, Melbourne WSR-88D, and geostationary satellites (GOES-I, J).

The last two bullets relate to the real-time subjective evaluation of MASS by forecasters and meteorologists at RWO, SMG, and NWS MLB.

- The distribution of model graphics as image products was too limiting because forecasters could not
    overlay MASS output with satellite images, observations, or other model output (from NCEP's NGM or Eta model),
    select other model variables not provided in the current image,
    change the location of cross sections, skew-t's, or station plots, and
    change contour intervals, colors, etc.

  In the future, gridded local model output could be sent back to forecasters so that they could develop and examine their own suite of products.

- Prior to the subjective evaluation, the AMU could have provided more thorough familiarization and training on MASS for RWO, SMG, and NWS MLB. This would have allowed the AMU to present more specific details regarding the model configuration, capabilities, product suite and availability, and to address questions, issues, concerns, etc. about MASS.

5.0   Future Work with MASS

This report concludes with a description of the future work planned or under consideration for MASS. As per Technical Directive 5-009 issued 29 February 1996, the AMU prepared a plan to continue running MASS with the changes and improvements recommended in Section 4.3. However, only one 24-h 11 km forecast will be run per day on the AMU's IBM RS/6000 Model 390. The reason for running just the 0000 UTC cycle is so that the Model 390 workstation can be used during the day for work on other AMU tasks. The 11 km run will be initialized from 0000 UTC data and start at approximately 2100 EST. The 24-h forecast will complete around 0600 EST and gridded output from MASS will be sent back to MIDDS. The AMU is waiting for MESO, Inc. to send version 5.9.3 of the MASS pre-processor and model. It is expected that real-time gridded MASS forecasts will be available in MIDDS beginning 1 May 1996.

The primary reason for continuing the MASS runs and sending output to MIDDS is to give RWO, SMG, and NWS MLB the opportunity to conduct additional, informal evaluation over a larger number of cases than was possible during 1995. However, the AMU cannot guarantee that daily MASS forecasts will be available since no additional labor is allocated for maintaining the real-time schedule. Nevertheless, the real-time run statistics suggest that MASS is reliable enough that it should not require much effort to keep it running during the 1996 warm season. Since all future work with MASS at this point is informal, the AMU will not archive forecasts nor do any further statistical verification. However, the AMU may examine MASS output as time permits during the real-time internal forecasting that will be done as part of the 29 km Eta model evaluation.

In preparation for the "mid-course correction" discussed in Section 4.2, the AMU identified a number of deficiencies affecting the modeling task that include

- Delayed access to NCEP gridded data,

- Insufficient communication bandwidth between the AMU PC and MIDDS, and

- No access to 915 MHz profiler data or digital NEXRAD data.

Except for access to digital NEXRAD data, these deficiencies should all be remedied as part of RWO's plan to upgrade MIDDS. The plan calls for the installation of a direct data line connecting RWO to NCEP and a separate AMU data server running TCP/IP which should be in place by December 1996. The access to digital NEXRAD data would require a high speed communication line connecting NWS MLB and RWO. The MIDDS upgrade has no current provision for access to digital NEXRAD data.

By the time the 29 Eta model evaluation is completed in March 1997, most if not all of these deficiencies will likely have been corrected. At that time, there is the possibility that the AMU could be tasked to resume work with MASS especially if further examination of MASS by RWO, SMG, or NWS MLB reveals that it has more added value that was not discovered as part of their limited subjective evaluation performed during the 1995 warm season.

6.0 References

Adler, R. F. and A. J. Negri, 1988: A satellite infrared technique to estimate tropical convective and stratiform rainfall. *J. Appl. Meteor.*, **27**, 30-51.

Anderson, J. R., E. E. Hardy, J. T. Roach and R. E. Witmer, 1976: A land use and land cover classification system for use with remote sensor data. U.S. Geological Survey Professional Paper 964. U.S. Government Printing Office, Washington, 28 pp.

Anthes, R. A., 1977: A cumulus parameterization scheme using a one-dimensional cloud model. *Mon. Wea. Rev.*, **105**, 270-286.

Barnes, S. L., 1964: A technique for maximizing details in numerical weather map analysis. *J. Appl. Meteor.*, **3**, 396-409.

Buzbee, B., 1993: Workstation clusters rise and shine. *Science*, **261**, 852-853.

Chang, J.-T., and P. J. Wetzel, 1991: Effects of spatial variations of soil moisture and vegetation on the evolution of a prestorm environment: A numerical case study. *Mon. Wea. Rev.*, **119**, 1368-1390.

Fischer, R. A., 1938: The statistical utilization of multiple measurements. *Annals of Eugenics*, **8**, 376-386.

Frank, W. M., and C. Cohen, 1987: Simulation of tropical convective systems. Part I: A cumulus parameterization. *J. Atmos. Sci.*, **44**, 3787-3799.

Fritsch, J. M., and C. F. Chappell, 1980: Numerical prediction of convectively driven mesoscale pressure systems. Part I: Convective parameterization. *J. Atmos. Sci.*, **37**, 1722-1733.

Gandin, L. S., 1963: *Objective analysis of meteorological fields*. Hydrometeorological Publishing House, 242 pp.

_____, and Murphy, A. S., 1992: Equitable skill scores for categorical forecasts. *Mon. Wea. Rev.*, **120**, 361-370.

Junker, N. W., J. E. Hoke and R. H. Grumm, 1989: Performance of NMC's regional models. *Wea. Forecasting*, **4**, 368-390.

Kaplan, M. L., J. W. Zack, V. C. Wong and J. J. Tuccillo, 1982: Initial results from a mesoscale atmospheric simulation system and comparisons with the AVE-SESAME I data set. *Mon. Wea. Rev.*, **110**, 1564-1590.

Kuo, H. L., 1965: On the formation and intensification of tropical cyclones through latent heat release by cumulus convection. *J. Atmos. Sci.*, **22**, 40-63.

Mahrt, L., and H. Pan, 1984: A two-layer model of soil hydrology. *Boundary-Layer Meteor.*, **29**, 1-20.

Manobianco, J., J. W. Zack, and G. E. Taylor, 1996: Workstation-based real-time mesoscale modeling designed for weather support to operations at the Kennedy Space Center and Cape Canaveral Air Station. *Bull. Amer. Meteor. Soc.*, **77**, in press.

McCumber, M. C., and R. A. Pielke, 1981: Simulation of the effects of surface fluxes of heat and moisture in a mesoscale numerical model. Part I: Soil layer. *J. Geophys. Res.*, **86**, 9929-9938.

MESO, 1993: MASS version 5.6 reference manual, 118 pp. [Available from MESO, Inc., 185 Jordan Road, Troy, NY 12180.]

Noilhan, J., and S. Planton, 1989: A simple parameterization of land surface processes for meteorological models. *Mon. Wea. Rev.*, **117**, 536-549.

Olson, D. A., N. W. Junker and B. Korty, 1995: Evaluation of 33 years of quantitative precipitation forecasting at NMC. *Wea. Forecasting*, **10**, 498-511.

Orlanski, I., 1976: A simple boundary condition for unbounded hyperbolic flows. *J. Comput. Phys.*, **21**, 251-269.

Perkey, D. J., and C. W. Kreitzberg, 1976: A time-dependent lateral boundary scheme for limited-area primitive equation models. *Mon. Wea. Rev.*, **104**, 745-755.

Pielke, R. A., G. Dalu, J. S. Snook, T. J. Lee and T. G. F. Kittel, 1991: Nonlinear influence of mesoscale land use on weather and climate. *J. Climate*, **4**, 1053-1069.

Sasamori, T., 1972: Radiative cooling calculation for application to general circulation experiments. *J. Appl. Meteor.*, **7**, 721-729.

Savijarvi, H., 1990: Fast radiation parameterization schemes for mesoscale and short-range forecast models. *J. Appl. Meteor.*, **29**, 437-447.

Schaefer, J. T., 1990: The critical success index as an indicator of warning skill. *Wea. Forecasting*, **5**, 570-575.

Schwartz, B., and S. G. Benjamin, 1995: A comparison of temperature and wind measurements from ACARS-equipped aircraft and rawinsondes. *Wea. Forecasting*, **10**, 528-544.

Spencer, P. L., F. H. Carr, and C. A. Doswell III, 1996: Diagnosis of an amplifying and decaying baroclinic wave using wind profiler data. *Mon. Wea. Rev.* **124**, 2099-223.

Stauffer, D. R., and N. L. Seaman, 1990: Use of four-dimensional data assimilation in a limited area mesoscale model. Part I: Experiments with synoptic-scale data. *Mon. Wea. Rev.*, **118**, 1250-1277.

_____,_____ and F. S. Binkowski, 1991: Use of four-dimensional data assimilation in a limited area mesoscale model. Part II: Effects of data assimilation within the planetary boundary layer. *Mon. Wea. Rev.*, **119**, 734-754.

Stephens, G. L., 1978: Radiation profiles in extended water clouds. II: Parameterization schemes. *J. Atmos. Sci.*, **35**, 2123-2132.

Xian, Z., and R. A. Pielke, 1991: The effects of width of land masses on the development of sea breezes. *J. Appl. Meteor.*, **30**, 1280-1304.

Young, S. H., and J. W. Zack, 1994: The use of non-standard data to improve the initialization of relative humidity in mesoscale models. Preprints: <u>Tenth Conference on Numerical Weather Prediction</u>, Portland, Amer. Meteor. Soc., 326-327.

Zack, J. W., K. T. Waight, S. H. Young, M. Ferguson, M. D. Bousquet and P. E. Price, 1993: Development of a mesoscale statistical thunderstorm prediction system. Final report to NASA under Contract No. NAS10-11670. 203 pp. [Available from MESO, Inc. 185 Jordan Road, Troy, NY 12180.]

Zhang, D.-L., 1989: The effect of parameterized ice microphysics on the simulation of vortex circulation with a mesoscale hydrostatic model. *Tellus*, **41A**, 132-147.

_____, and R. A. Anthes, 1982: A high resolution model of the planetary boundary layer - sensitivity tests and comparisons with SESAME-79 data. *J. Appl. Meteor.*, **21**, 1594-1609.

_____, and J. M. Fritsch, 1986: Numerical simulation of the meso-β-scale structure and evolution of the 1977 Johnstown flood. Part I: Model description and verification. *J. Atmos. Sci.*, **43**, 1913-1943.

Zupanski, D., and F. Mesinger, 1995: Four-dimensional variational assimilation of precipitation data. *Mon. Wea. Rev.*, **123**, 1112-1127.

NOTICE